Effects of Lateral Inhomogeneity and Non-hydrostatic Pre-stress of Earth on Tidal Gravity

Zhenyu Wang[1], Guangyu Fu[2,3]

[1] Institute of Geophysics, China Earthquake Administration, Beijing 100081, China

[2] School of Geophysics and Information Technology, China University of Geosciences, Beijing 100083, China

[3] Institute of Earthquake Forecasting, China Earthquake Administration, Beijing 100036, China

Corresponding author: Guangyu Fu (fugy@ief.ac.cn)

Key Points:

- Expressions for calculating the effects of non-hydrostatic pre-stress on tidal gravity with perturbation method are presented
- Global variations of theoretical semidiurnal tidal gravimetric factors are calculated using a real three-dimensional Earth model
- This study obtained theoretical values with improved matching to superconducting gravimeter measurements compared to traditional theory

Abstract

Tidal theory for a three-dimensional Earth model stipulates that non-hydrostatic pre-stress arises from the transition from a spherically-symmetrical model to an asymmetrical model when introducing asymmetrical density increments. The contribution of non-hydrostatic pre-stress on tidal gravity has been neglected in previous studies since the effects of density increments are assumed to be smaller than those of rheology parameter increments. This study for the first time presents expressions for calculating the effects of non-hydrostatic pre-stress on tidal gravity and develops the tidal theory for a three-dimensional Earth model. The expressions are verified with the simple ocean-land model after which the effects of non-hydrostatic pre-stress are calculated using the real Earth model GyPSuM. The results suggest that although the effects of non-hydrostatic pre-stress are less than those of seismic wave velocity disturbance, the contribution to final results is significant and should not be neglected. By considering the collective contributions of seismic wave velocity disturbance, density disturbance, and non-hydrostatic pre-stress, the global theoretical variation of M2 semidiurnal gravimetric factors is obtained, and varies from −0.16% to 0.09% compared to those in a layered Earth model. M2 gravimetric factors measured by superconducting gravimeters worldwide are collected and compared to the theoretical results of this study. Theoretical values generated by the three-dimensional tidal theory for 11 of 14 stations show an improved match to measurements compared to those of traditional theory, which further verifies the accuracy of the formulae presented by this study.

Plain Language Summary

Tidal gravity has profound influences on daily life and has been measured accurately by gravimeters. A theory for calculating the theoretical tidal gravity is developed here to support these measurements. According to previous investigations on the theory, many factors affect tidal gravity, including Earth's ellipticity, inelasticity, and lateral inhomogeneity. However, the effect of the nonequilibrium state of the Earth on tidal gravity has not been established as researchers generally consider that its effects are too small to detect. Consequently, these effects are neglected and the analytical expressions for calculating the effects have not yet been presented. This paper proposes an approach to calculate these effects, which is validated through a numerical test. The components of tidal gravity are also computed using a real three-dimensional Earth model. The three-dimensional results generated by this study show improved consistency with measurements compared to those of traditional theory, suggesting that the effects of nonequilibrium cannot be ignored.

1 Introduction

Tides induced by gravitational attraction of the sun and moon constantly affect the shape and gravity field of Earth. The improvements in measurement techniques allow increasingly precise monitoring of periodic changes in geoid and gravity, which are concomitant with solid tides. The precision of the global positioning system (GPS) and very long baseline interferometry (VLBI) in representing surface deformation is up to 1 mm (Petrov & Boy, 2004), and the iGrav superconducting gravimeter can detect gravity changes of 1 nms^{-2} (Fores et al., 2016). These observations are of importance for investigating Earth's internal structures and dynamic processes (Yuan et al., 2013). Correspondingly, tidal theories have been developed to interpret and support the observations.

The first studies on tidal theory occurred in the early 20th century, with Love (1909) pioneering a method for calculating the tidal deformation of a spherically-stratified and nonrotating Earth. Longman (1963), Saito (1967), Farrell (1972), and Takeuchi & Saito (1972) gradually developed the tidal theory by taking account of spherical symmetry, elasticity, and isotropy of the Earth. Wahr (1981) presented the expressions for computing tidal deformation of a rotating ellipsoid, the influence of which on tidal observations is ~1%. Using Wahr's work (1981) as a basis, Wahr & Bergen (1986) and Dehant (1987) considered the inelastic mantle, and the gravimetric factors evaluated by Dehant (1987) turned out to be 1.4%–3% larger than those of the elastic mantle. de Vries & Wahr (1991) studied the effects of a solid inner core and non-hydrostatic structure on the Earth's tides. Dehant et al. (1999) calculated tidal gravimetric factors for two rotating, non-spherical Earth models and determined that the results of an inelastic Earth model with a non-hydrostatic initial state are closer to measurements compared to those of an elastic Earth model in hydrostatic equilibrium. Lau & Faul (2019) developed and validated the method of Wahr & Bergen (1986) using measurements and calculated the effects of inelasticity on tidal gravity. The majority of the aforementioned studies did not consider the direct effects of lateral inhomogeneity in the mantle. Although some studies considered mantle convection induced by lateral inhomogeneity, the treatments on rheology parameters remained one-dimensional (Dziewonski & Anderson, 1981).

In fact, the occurrence of plumes, volcanoes, and other dynamic phenomena demonstrate that the interior of the Earth is far from homogeneous but full of large lateral variations. As a result, scientists have used the perturbation or finite element methods to study solid tidal gravity in a three-dimensional Earth model. Métivier et al. (2006) used a spectral element method to develop a model of elastogravitational deformation which considers lateral inhomogeneity as well as non-hydrostatic pre-stress. Métivier et al. (2007) used this elastogravitational model to study the effects of plumes on solid tidal gravity. Although Molodenskiy (1980) presented expressions for determining changes to the tidal gravimetric factor induced by lateral inhomogeneity based on the perturbation method, only the effects of seismic waves have been considered. Molodenskii & Kramer (1980) based on the work of Molodenskiy (1980) to evaluate the changes in gravimetric factor for a simple laterally-heterogeneous ocean-land model. Wang (1991) studied tidal deformations on a rotating, spherically-asymmetrical, visco-elastic and laterally-heterogeneous Earth model. Fu & Sun (2007) developed the tidal theory by determining the effects of laterally varying densities in the mantle on tidal gravity, and considered that the effects are comparable with those of laterally-varying seismic wave velocities. Qin et al. (2014) proposed a semi-analytical method to compute solid tidal gravity for a laterally-heterogeneous Earth model. These aforementioned studies generally neglected the effects of non-hydrostatic pre-stress. Although Métivier et al. (2007) evaluated the effects of non-hydrostatic pre-stress based on the spectral element method, analytical solutions have not yet been derived by studies based on the perturbation method. Therefore, this component of tide theory poses a challenge that needs to be discussed.

The aim of this study is to present formulae for representing the effects of non-hydrostatic pre-stress on tidal gravimetric factors with the use of the perturbation method and to determine whether the effects of non-hydrostatic pre-stress are negligible. The expressions for computing the effects of non-hydrostatic pre-stress on tidal gravimetric factors are first presented, following which a numerical test is performed using a simple ocean-land model. Finally the M2 components of semidiurnal tidal gravimetric factors are computed using a three-dimensional inhomogeneous model GyPSuM (Simmons et al., 2010), and the results are compared to

measurements of 14 superconducting gravimeters distributed globally. The theoretical values derived from a three-dimensional Earth model are closer to observations compared to values derived from a layered Earth model, and non-hydrostatic pre-stress makes a considerable contribution to the final results and is therefore not negligible.

2 Tidal Theory in a Three-Dimensional Inhomogeneous Earth Model Based on the Perturbation Method

The tidal theory presented in the current study starts from a system of equations describing an elastic, self-gravitational, and spherically-symmetrical Earth model. The equilibrium, constitutive, and Poisson equations (Farrell, 1972; Takeuchi & Saito, 1972) are:

$$L(\boldsymbol{u},\Psi) = \rho g \boldsymbol{e}_r(\nabla\cdot\boldsymbol{u}) - \rho\nabla(\Psi + g u_r) + \nabla\cdot\tau = 0 \tag{1}$$

$$\tau = \lambda \mathbf{I}\nabla\cdot\boldsymbol{u} + \mu(\nabla\boldsymbol{u} + (\nabla\boldsymbol{u})^T) \tag{2}$$

$$\nabla^2\Psi = -4\pi G(\delta\rho) = 4\pi G\nabla\cdot(\rho\boldsymbol{u}) \tag{3}$$

In equations 1-3, $\boldsymbol{u}$ is the displacement vector, Ψ is the gravitational potential changes during deformation, ρ is density, g is gravity, $\boldsymbol{e}$ is unit vector, subscript r indicates the radial direction, τ is stress tensor, λ and μ are Lame's constants, and G is Newton's gravitational constant. Equations 1-3 are reduced to dimensionless form for convenience. The values of the rheology parameter λ_0, density ρ_0 at the center and gravity g_0 on the surface of the Earth are denoted as the unit rheology parameter, unit density, and unit gravity, respectively.

Displacement $\boldsymbol{u}$, stress tensor component $\tau\cdot\boldsymbol{e}_r$, and potential changes Ψ during tidal deformation can be expanded into a series of spherical harmonic functions:

$$\boldsymbol{u}^0 = \sum_{n_0=0}^{\infty}\sum_{m_0=-n_0}^{n_0}\boldsymbol{u}^{n_0m_0} = \sum_{n_0=0}^{\infty}\sum_{m_0=-n_0}^{n_0}\left[y_1(r;n,m)\boldsymbol{R}_{n_0}^{m_0}(\theta,\phi) + y_3(r;n,m)\boldsymbol{S}_{n_0}^{m_0}(\theta,\phi)\right] \tag{4}$$

$$\tau^0\cdot\boldsymbol{e}_r = \sum_{n_0=0}^{\infty}\sum_{m_0=-n_0}^{n_0}\boldsymbol{T}^{n_0m_0} = \sum_{n_0=0}^{\infty}\sum_{m_0=-n_0}^{n_0}\left[y_2(r;n,m)\boldsymbol{R}_{n_0}^{m_0}(\theta,\phi) + y_4(r;n,m)\boldsymbol{S}_{n_0}^{m_0}(\theta,\phi)\right] \tag{5}$$

$$\Psi^0 = \sum_{n_0=0}^{\infty}\sum_{m_0=-n_0}^{n_0}\Psi^{n_0m_0} = \sum_{n_0=0}^{\infty}\sum_{m_0=-n_0}^{n_0}y_5(r;n,m)Y_{n_0}^{m_0}(\theta,\phi) \tag{6}$$

The subscript and superscript 0 indicate variables of the spherically-symmetrical model, distinct from those of the spherically-asymmetrical model (see below). The Toroidal component

of the model is not considered as Fu & Sun (2007) have confirmed that this component makes no contribution to changes in gravity. In equations 4 and 5,

$$\boldsymbol{R}_{n_0}^{m_0}(\theta,\phi) = \boldsymbol{e}_r Y_{n_0}^{m_0}(\theta,\phi) \tag{7}$$

$$\boldsymbol{S}_{n_0}^{m_0}(\theta,\phi) = \left[\boldsymbol{e}_\theta \frac{\partial}{\partial\theta} + \boldsymbol{e}_\phi \frac{1}{\sin\theta}\frac{\partial}{\partial\phi}\right] Y_{n_0}^{m_0}(\theta,\phi) \tag{8}$$

$$Y_{n_0}^{m_0}(\theta,\phi) = P_{n_0}^{m_0}(\cos\theta)\begin{cases}\cos m_0\phi \\ \sin m_0\phi\end{cases} \tag{9}$$

In equations 7-9, $\boldsymbol{e}_r$, $\boldsymbol{e}_\theta$, and $\boldsymbol{e}_\phi$ are unit vectors, $P_{n_0}^{m_0}(\cos\theta)$ is the Legendre function for degree n_0 and order m_0. The use of sine or cosine in equation 9 is determined in Section 4. $y_6(r)$ is defined as follows according to Longman (1963):

$$y_6(r;n,m) = \dot{y}_5(r;n,m) - 4\pi G\rho y_1(r;n,m) \tag{10}$$

In equation 10, the dot indicates a derivative with regard to r, coefficients $y_i(r;n,m), i = 1,\dots,6$ for specific problems (not confined to tide) can be determined using the boundary conditions by substituting equations 4-6 and 10 into equations 1-3, as shown in Appendix A.

Gravity variations $\Delta g(r,\theta,\phi)$ consist of the radial derivative of potential changes Ψ and the contribution of displacement. On the free surface:

$$\Delta g(a,\theta,\phi) = -\frac{\partial\Psi}{\partial r}\bigg|_a - \beta u_r(a,\theta,\phi) \tag{11}$$

In equation 11, β denotes the free-air gravity gradient, a is the surface radius, and $u_r(a,\theta,\phi)$ is the radial displacement.

According to Sun & Okubo (1993):

$$-\frac{\partial\Psi}{\partial r}\bigg|_a = \frac{g_0 UdS}{a^3}\sum_{n=0}^{\infty}\sum_{m=-n}^{n}[(n+1)y_5(a;n,m)]Y_n^m(\theta,\phi) \tag{12}$$

equation 11 may be rewritten as:

$$\Delta g(a,\theta,\phi) = \frac{g_0 UdS}{a^3}\sum_{n=0}^{\infty}\sum_{m=-n}^{n}[(n+1)y_5(a;n,m)]Y_n^m(\theta,\phi) - \frac{\beta UdS}{a^2}\sum_{n=0}^{\infty}\sum_{m=-n}^{n}[y_1(a;n,m)]Y_n^m(\theta,\phi)$$

(13)

for $\beta = \frac{2g_0}{a}$, equation 13 becomes:

$$\Delta g(a,\theta,\phi) = \frac{g_0 UdS}{a^3}\sum_{n=0}^{\infty}\sum_{m=-n}^{n}[(n+1)y_5(a;n,m)]Y_n^m(\theta,\phi) - \frac{2g_0 UdS}{a^3}\sum_{n=0}^{\infty}\sum_{m=-n}^{n}[y_1(a;n,m)]Y_n^m(\theta,\phi)$$

(14)

Using the unit of $g_0 UdS = 1$ and $a = 1$, equation 14 is simplified as:

$$\Delta g(a,\theta,\phi) = \sum_{n=0}^{\infty}\sum_{m=-n}^{n}[(n+1)y_5(1;n,m) - 2y_1(1;n,m)]Y_n^m(\theta,\phi)$$

(15)

Equation 15 shows that variations in gravity resulting from the tide can be computed by coefficients y_1 and y_5. Since the Earth is in reality not spherically-symmetrical, the effects of lateral inhomogeneity must be considered. The most significant effect is that adding the asymmetric increments $\delta\lambda(r,\theta,\phi)$, $\delta\mu(r,\theta,\phi)$, and $\delta\rho(r,\theta,\phi)$ to the spherically-symmetrical model increases the difficulty in expanding $\boldsymbol{u}$ and Ψ. Consequently, the variations in gravity cannot be directly computed. Molodenskiy (1977) resolved this problem based on the perturbation method by separating the effects of asymmetrical increments from those of the spherically-symmetrical model, and presented analytical expressions for computing the effects of asymmetrical increments on tidal gravity using auxiliary solutions. According to this method:

$$\boldsymbol{u} = \boldsymbol{u}^0 + \delta\boldsymbol{u}$$

(16)

$$\Psi = \Psi^0 + \delta\Psi$$

(17)

In equations 16 and 17, $\boldsymbol{u}^0$ and Ψ^0 are the unperturbed solutions for the spherically-symmetrical model, $\delta\boldsymbol{u}$ and $\delta\Psi$ are the perturbed solutions for asymmetrical increments.

In previous works, researchers considered that the Earth is under non-hydrostatic state, and non-hydrostatic pre-stress is considered in their equilibrium equations (Métivier et al., 2006; Métivier et al., 2007; Lau et al., 2015; Lau & Faul, 2019). Differing from these works, the current study is based on the perturbation method, which focuses on the effects of the three-dimensional lateral inhomogeneity of the Earth. The key of this method is to assume that the real Earth is the summation of a spherically-symmetrical Earth under the hydrostatic state and the small lateral variations of density and elastic moduli. The perturbation method works if the lateral variations are small. In this framework, the non-hydrostatic stress arises when adding the disturbances to the unperturbed one-dimensional Earth, namely, transforming a spherically-symmetrical Earth to a spherically-asymmetrical one. Consequently, we begin the mathematical work with the equilibrium equation under the hydrostatic state. The perturbation method is also

used by Molodenskiy (1980), Molodenskii & Kramer (1980), Wang (1991), and Fu & Sun (2007), and has been tested valid.

Similar to equations 4 and 6:

$$\delta \boldsymbol{u} = \sum_{n=0}^{\infty} \sum_{m=-n}^{n} \delta \boldsymbol{u}^{nm} = \sum_{n=0}^{\infty} \sum_{m=-n}^{n} [y_1^*(r;n,m)\boldsymbol{R}_n^m(\theta,\phi) + y_3^*(r;n,m)\boldsymbol{S}_n^m(\theta,\phi)] \tag{18}$$

$$\delta \Psi = \sum_{n=0}^{\infty} \sum_{m=-n}^{n} \delta \Psi^{nm} = \sum_{n=0}^{\infty} \sum_{m=-n}^{n} y_5^*(r;n,m) Y_{n_0}^{m_0}(\theta,\phi) \tag{19}$$

In equations 18 and 19, $y_i^*(r;n,m)$ are the expanded coefficients of perturbed solutions. The effects of lateral inhomogeneity on gravity can be obtained once the coefficients are determined and substituted into equation 15. In contrast to the coefficients of unperturbed solutions, those of perturbed solutions cannot be directly computed using the method shown in Appendix A since the boundary conditions of the coefficients are uncertain. Molodenskiy (1977) proposed a method to determine the coefficients basing on the Betti Reciprocal theorem and the perturbation method, where by reformulating equations 1 and 3:

$$L_i(\delta \boldsymbol{u}, \delta \Psi) + \delta L_i(\boldsymbol{u}^0, \Psi^0) = 0 \tag{20}$$

$$\Delta(\delta \Psi) = 4\pi G \nabla \cdot (\delta \rho \boldsymbol{u} + \rho \delta \boldsymbol{u}) \tag{21}$$

In equations 20 and 21, the subscripts $i = 1,2,3$ are the three components of the coordinate system. Here, the auxiliary solutions $\boldsymbol{u}_i^j$ and $\Psi^j, j = 1,2,3$ are defined, which are displacement and potential changes of the unperturbed Earth resulting from external forces, respectively. These auxiliary solutions have no physical significance, although their forms are similar to those of pressure $(j = 1)$, shear $(j = 2)$, and tide $(j = 3)$ since they are purely defined to determine the perturbed solutions. The auxiliary solutions satisfy the following equations:

$$L_i\left(\boldsymbol{u}^j, \Psi^j\right) = 0 \tag{22}$$

$$\Delta \Psi^j = 4\pi G \nabla \cdot \left(\rho \boldsymbol{u}^j\right) \tag{23}$$

By multiplying equations 20 and 22 by u_i^j and $-\delta u_i$, the results over three directions of $i = 1,2,3$ are summarized, and by integrating the result over the volume:

$$\iiint u_i^j \, \delta L_i(\boldsymbol{u}^0, \Psi^0) dv + I = 0 \tag{24}$$

Therein:

$$\delta L_i(\boldsymbol{u}^0, \Psi^0) = \delta\rho[g\boldsymbol{e}_r(\nabla\cdot\boldsymbol{u}^0) - \nabla_i(\Psi^0 + gu_r^0)] + \rho[\delta g\boldsymbol{e}_r(\nabla\cdot\boldsymbol{u}^0) - \nabla_i(\delta g u_r^0)] + \nabla_k(\delta p_{ik} + \delta\tau_{ik})$$

(25)

$$I = \iiint \left[u_i^j L_i(\delta\boldsymbol{u}, \delta\Psi) - \delta u_i L_i\left(\boldsymbol{u}^j, \Psi^j\right)\right] dv$$

(26)

In equations 25 and 26, δg is the perturbation of gravity resulting from $\delta\rho$, $\delta p_{ik} = \delta\mu\left(\frac{\partial u_i^0}{\partial x_k} + \frac{\partial u_k^0}{\partial x_i}\right) + \delta\lambda\nabla\cdot(\boldsymbol{u}^0)\delta_{ik}$, denotes perturbation of stress under the hydrostatic state. The initial stress state moves out of equilibrium once perturbation of density is introduced. As a result, the deviation of non-hydrostatic stress $\delta\tau_{ik}$ from hydrostatic stress due to perturbation must be considered. Omitting tedious mathematical work (see more details in Molodenskiy, 1977), equation 26 becomes:

$$I = \frac{4\pi(n+m)!}{\varepsilon_m(2n+1)(n-m)!} \cdot \left[-y_1^*(1;n,m)y_2^j(1) - n(n+1)y_3^*(1;n,m)y_4^j(1) - \frac{1}{4\pi G}y_5^*(1;n,m)y_6^j(1)\right] + \iiint \Psi^j\nabla\cdot(\delta\rho\boldsymbol{u}^0)\,dv + \iint\left(u_i^j\delta p_{ik} - \Psi^j u_k^0\delta\rho\right)dS_k$$

(27)

Therein:

$$\varepsilon_m = \begin{cases} 1 & m = 0 \\ 2 & m \neq 0 \end{cases}$$

$$\delta p_{ik}|_S = -\left[\delta\mu\left(\frac{\partial u_i^0}{\partial x_k} + \frac{\partial u_k^0}{\partial x_i}\right) + \delta\lambda\nabla\cdot(\boldsymbol{u}^0)\delta_{ik}\right]\Bigg|_S$$

$$dS_k = \frac{x_k}{r}dS$$

According to the divergence theorem, the last term on the right-hand side of equation 27 becomes:

$$\iint\left(u_i^j\delta p_{ik} - \Psi^j u_k^0\delta\rho\right)dS_k = \iiint\nabla_k\cdot\left(-u_i^j\delta p_{ik} - \Psi^j u_k^0\delta\rho\right)dv = \iiint\left\{-\frac{\partial u_i^j}{\partial x_k}\left[\delta\mu\left(\frac{\partial u_i^0}{\partial x_k} + \frac{\partial u_k^0}{\partial x_i}\right) + \delta\lambda\nabla\cdot(\boldsymbol{u}^0)\delta_{ik}\right] - u_i^j\nabla_k\delta p_{ik} - \Psi^j\nabla\cdot(\delta\rho\boldsymbol{u}^0) - \delta\rho\left(\boldsymbol{u}^0, \nabla\Psi^j\right)\right\}dv$$

(28)

In equation 28, $\left(\boldsymbol{u}^0, \nabla\Psi^j\right)$ is the inner product. By substituting equations 25, 27, and 28 into equation 24 through simple manipulations:

$$F^j(\delta\rho, \delta\mu, \delta\lambda, \delta\tau) = \frac{4\pi(n+m)!}{\varepsilon_m(2n+1)(n-m)!} \cdot \left[y_1^*(1;n,m)y_2^j(1) + n(n+1)y_3^*(1;n,m)y_4^j(1) + \frac{1}{4\pi G}y_5^*(1;n,m)y_6^j(1)\right] \tag{29}$$

Where:

$$F^j(\delta\rho, \delta\mu, \delta\lambda, \delta\tau) = \iiint \left\{-\delta\rho\left(\boldsymbol{u}^0, \nabla\Psi^j\right) + u_i^j \delta L_{i\rho}(\boldsymbol{u}^0, \Psi^0) - \delta\mu\left(\frac{\partial u_i^0}{\partial x_k} + \frac{\partial u_k^0}{\partial x_i}\right)\frac{\partial u_i^j}{\partial x_k} - \delta\lambda\nabla\cdot(\boldsymbol{u}^0)\nabla \cdot \left(\boldsymbol{u}^j\right) + u_i^j\nabla_k\delta\tau_{ik}\right\} dv \tag{30}$$

$$\delta L_{i\rho}(\boldsymbol{u}^0, \Psi^0) = \delta\rho[g\boldsymbol{e}_r(\nabla\cdot\boldsymbol{u}^0) - \nabla_i(\Psi^0 + gu_r^0)] + \rho[\delta g\boldsymbol{e}_r(\nabla\cdot\boldsymbol{u}^0) - \nabla_i(\delta g u_r^0)] \tag{31}$$

According to equation 29, the following expressions can be considered as boundary conditions for auxiliary solutions to calculate the perturbed solutions $y_i^*(1;n,m)$.

$$\begin{aligned} &1)\ j=1 \quad y_2^1(1)=1 \qquad y_4^1(1)=0 \qquad y_6^1(1)=0 \\ &2)\ j=2 \quad y_2^2(1)=0 \quad y_4^2(1)=\frac{1}{n(n+1)} \quad y_6^2(1)=0 \\ &3)\ j=3 \quad y_2^3(1)=0 \qquad y_4^3(1)=0 \qquad y_6^3(1)=4\pi G \end{aligned} \tag{32}$$

The following can be derived:

$$F^j(\delta\rho, \delta\mu, \delta\lambda, \delta\tau) = c(n,m)\begin{cases} y_1^*(1;n,m), & j=1 \\ y_3^*(1;n,m), & j=2 \\ y_5^*(1;n,m), & j=3 \end{cases} \tag{33}$$

$$c(n,m) = \iint \left(Y_n^m(\theta,\phi)\right)^2 dS = \frac{4\pi(n+m)!}{\varepsilon_m(2n+1)(n-m)!} \tag{34}$$

The boundary conditions shown in equation 32 are similar to those of pressure, shear, and tide problems, respectively. But actually auxiliary solutions have no physical significance. For the right-hand side of equation 33, only $y_1^*(1;n,m)$ and $y_5^*(1;n,m)$ affect gravity. Once these

two terms are determined and substituted into equation 15, the effects of lateral inhomogeneity on surface gravity can be obtained. It should be noted that the special cases of $n = 0$ and $n = 1$ require further treatment, with a more detailed description in Fu & Sun (2007).

3 Effects of Non-hydrostatic Pre-stress

As mentioned above, to determine $y_i^*(1; n, m)$, obtaining the quadrature $F^j(\delta\rho, \delta\mu, \delta\lambda, \delta\tau)$ is crucial. $F^j(\delta\rho, \delta\mu, \delta\lambda, \delta\tau)$ can be decomposed into four parts as:

$$F^j(\delta\rho, \delta\mu, \delta\lambda, \delta\tau) = F^j(\delta\rho) + F^j(\delta\mu) + F^j(\delta\lambda) + F^j(\delta\tau) \tag{35}$$

In equation 35, $F^j(\delta\rho), F^j(\delta\mu), F^j(\delta\lambda)$, and $F^j(\delta\tau)$ correspond to the effects of $\delta\rho$, $\delta\mu$, $\delta\lambda$, and $\delta\tau$, respectively. The first three terms on the right-hand side of equation 35 have been meticulously defined by Molodenskiy (1980) and Fu & Sun (2007). The present study addresses the expressions directly as below:

$$F_{nm}^j(\delta\lambda) = -\sum_{l=0}^{N_e}\sum_{p=-l}^{l} A_{lpnmn_0m_0}\int_0^1 \lambda_{lp}(r)x_{nn_0}^{(1)(j)}(r)dr \tag{36}$$

$$F_{nm}^j(\delta\mu) = -\sum_{l=0}^{N_e}\sum_{p=-l}^{l} A_{lpnmn_0m_0}\int_0^1 r^{n+n_0}\mu_{lp}(r)\left[x_{nn_0}^{(2)(j)}(r) + nn_0x_{nn_0}^{(3)(j)}(r) + nn_0(nn_0 - n_0 - n + 3)x_{nn_0}^{(4)(j)}(r)\right]dr \tag{37}$$

$$F_{nm}^j(\delta\rho) = -\sum_{l=0}^{N_e}\sum_{p=-l}^{l} A_{lpnmn_0m_0}\int_0^1 \rho(r)\left\{\gamma_{lp}^1(r)\left[x_{nn_0}^{(5)(j)}(r) + nn_0x_{nn_0}^{(6)(j)}(r)\right] + \gamma_{lp}^2(r)\left[x_{nn_0}^{(7)(j)}(r) - lx_{nn_0}^{(8)(j)}(r) + nn_0x_{nn_0}^{(9)(j)}(r) + lnx_{nn_0}^{(10)(j)}(r)\right] + \gamma_{lp}^3(r)x_{nn_0}^{(11)(j)}(r)\right\}dr \tag{38}$$

$$A_{lpnmn_0m_0} = \iint Y_l^p(\theta,\phi)Y_n^m(\theta,\phi)Y_{n_0}^{m_0}(\theta,\phi)dS \tag{39}$$

$$\begin{cases}\gamma^1 = \delta\rho/\rho \\ \gamma^2 = \delta g/g \\ \gamma^3 = \delta\dot{g}/\dot{g}\end{cases} \tag{40}$$

In equations 36-38, $\lambda_{lp}(r)$, $\mu_{lp}(r)$, $\gamma_{lp}^{1}(r)$, $\gamma_{lp}^{2}(r)$, and $\gamma_{lp}^{3}(r)$ are spherical harmonic expansion coefficients for $\delta\lambda$, $\delta\mu$, $\delta\rho/\rho$, $\delta g/g$, and $\delta\dot{g}/\dot{g}$, respectively, N_e is the convergent degree of the three-dimensional Earth model, n and m are the expansion degree and order for auxiliary solutions, respectively, and n_0 and m_0 are the degree and order for the tidal component of interest, respectively. The treatment of $A_{lpnmn_0m_0}$ is shown in Appendix B whereas definitions of coefficients $x_{nn_0}^{(i)(j)}(r)$ can be found in Appendix C.

The majority of previous studies considered the effects of non-hydrostatic pre-stress to be negligible. Molodenskii & Kramer (1980) and Vermeersen & Vlaar (1991) concluded that the effects of non-hydrostatic pre-stress resulting from density disturbance together with the effects of density disturbance can be neglected since they considered the density disturbance to be much lower than seismic wave velocity disturbance. Since Geller (1988) and Fu & Sun (2007) assumed that the time scales of tidal deformation are much lower than those of dynamic processes, they considered the Earth to be in a quasi-equilibrium state and that non-hydrostatic pre-stress is negligible. In contrast, Métivier et al. (2007) computed the effects of dynamic topography which is related to non-hydrostatic pre-stress based on the spectral element method, and argued that the effects are not negligible. On the other hand, the majority of studies based on the perturbation method have not quantitatively discussed the effects of non-hydrostatic pre-stress or provided analytical expressions. The current study presents the expressions for the effects of non-hydrostatic pre-stress in this section to develop the theory and assesses whether the effects are negligible in subsequent sections.

Given the form of equation 1, the equilibrium equation can be transformed into perturbed equation as follows:

$$\begin{aligned}\delta L_i(\boldsymbol{u}^0,\Psi^0) = {} & \delta\rho[g\boldsymbol{e}_r(\nabla\cdot\boldsymbol{u}^0)-\nabla_i(\Psi^0+gu_r^0)]+\rho[\delta g\boldsymbol{e}_r(\nabla\cdot\boldsymbol{u}^0)-\nabla_i(\delta gu_r^0)]\\ & +\nabla_k(\delta p_{ik}+\delta\tau_{ik})\end{aligned} \tag{41}$$

In equation 41, $\delta L_i(\boldsymbol{u}^0,\Psi^0)$ is the variation of the i-th component of the operator L, corresponding to the transition from a spherically-symmetrical distribution to a spherically-asymmetrical distribution. δp_{ik} is the disturbance of hydrostatic stress. The term related to non-hydrostatic stress $\delta\tau_{ik}$ is resulted from taking account of disturbances. The initial hydrostatic stress p^0 and initial non-hydrostatic stress τ^0 are defined, which satisfies:

$$p^0\mathbf{I}+\tau^0 = T^0 \tag{42}$$

$$p^0 = \frac{1}{3}\mathrm{tr}T^0 \tag{43}$$

In equation 42, $\mathbf{I}$ is the identity matrix. Following the approach of Dahlen (1972), the constitutive equations are:

$$T_{iki'k'} = C_{iki'k'}\sigma_{i'k'}+\frac{1}{2}\left(T_{i'k'}^0\delta_{ik}-T_{ik}^0\delta_{i'k'}\right)\sigma_{i'k'}$$

$$C_{iki'k'} = \lambda\delta_{ik}\delta_{i'k'}+\mu(\delta_{ii'}\delta_{kk'}+\delta_{ik'}\delta_{ki'})$$

$$\sigma_{ik} = \frac{1}{2}\left(\frac{\partial u_i}{\partial x_k} + \frac{\partial u_k}{\partial x_i}\right) \tag{44}$$

If initial stress is hydrostatic, namely $T^0 = p^0\mathbf{I}$, equation 44 can be simplified as:

$$T_{ik} = E_{ik} = C_{iki'k'}\sigma_{i'k'} \tag{45}$$

Equation 45 is equivalent to equation 2.

According to equation 44, δp_{ik} and $\delta\tau_{ik}$ can be written as:

$$\delta p_{ik} = \delta\mu\left(\frac{\partial u_i^0}{\partial x_k} + \frac{\partial u_k^0}{\partial x_i}\right) + \delta\lambda\nabla\cdot(\boldsymbol{u}^0)\delta_{ik} \tag{46}$$

$$\delta\tau_{ik} = \frac{1}{2}\delta\left(T_{i'k'}^0\delta_{ik} - T_{ik}^0\delta_{i'k'}\right)\sigma_{i'k'} \tag{47}$$

In equations 47, $\delta\left(T_{i'k'}^0\delta_{ik} - T_{ik}^0\delta_{i'k'}\right)$ is the variation of initial stress corresponding to the introduced disturbance of Lame's constants. According to Dahlen (1972):

$$\frac{1}{2}\left(T_{i'k'}^0\delta_{ik} - T_{ik}^0\delta_{i'k'}\right) = C_{iki'k'} - B_{i'k'ik} \tag{48}$$

The conclusion of Dahlen (1972) has been revised by recent works (Tromp & Trampert, 2018; Maitra & Al-Attar, 2020). Dahlen (1972) considered that the seismic wave speeds are isotropic, whereas Tromp & Trampert (2018) porposed that the seismic wave speeds are various under the effect of induced stress. The present study also takes account of the seismic wave speed disturbances, and these disturbances are added to a one-dimensional Earth model. Consequently, the expressions of Dahlen (1972) are suitable for our research. It's in common that both this work and Tromp & Trampert (2018) considered the variations of stresses are not independent with the variations of elastic moduli. Under the framework of perturbation method, the variations appear in the perturbation equations in the present study, rather than in the constitutive equations as Tromp & Tampert (2018) did. We will take into consideration of the recent works (Tromp & Trampert, 2018; Maitra & Al-Attar, 2020) in our future research.

According to equation 48, the term $\delta\left(T_{i'k'}^0\delta_{ik} - T_{ik}^0\delta_{i'k'}\right)$ consists of disturbance of initial hydrostatic stress $\delta C_{iki'k'}$ and disturbance of initial non-hydrostatic stress $\delta B_{i'k'ik}$. If $B_{i'k'ik}$ is treated as the first order perturbation resulting from the transition from a spherically-symmetrical model to a spherically-asymmetrical model, $\delta B_{i'k'ik}$ can be considered as the negligible second-order term, namely, $\delta\tau_{ik} = \delta C_{iki'k'} = \mu\gamma^1\left(\frac{\partial u_i^0}{\partial x_k} + \frac{\partial u_k^0}{\partial x_i}\right) + \lambda\gamma^1\nabla\cdot(\boldsymbol{u}^0)\delta_{ik}$. By substituting this expression into the last term of equation 30, the following equation is obtained:

$$F_{nm}^{j}(\delta\tau) = \iiint u_i^j \, \nabla_k \delta\tau_{ik} dv = \iiint u_i^j \, \nabla_k \left[\mu\gamma^1 \left(\frac{\partial u_i^0}{\partial x_k} + \frac{\partial u_k^0}{\partial x_i} \right) + \lambda\gamma^1 \nabla \cdot (\boldsymbol{u}^0) \delta_{ik} \right] dv \tag{49}$$

Note that the non-hydrostatic stress arises because of adding the lateral density disturbances to the spherically-symmetrical Earth. Therefore, it's self-consistant that we relate the effects of non-hydrostatic pre-stress to the disturbances of density (Molodenskiy, 1980). The usages of $\mu\gamma^1$ and $\lambda\gamma^1$ in the above equation are followed the equations 42 and 43 of Fu & Sun (2007). According to Appendix D, the expression for $F^j(\delta\tau)$ can be written as follows:

$$\begin{aligned} F_{nm}^{j}(\delta\tau) = \sum_{l=0}^{N_e} \sum_{p=-l}^{l} A_{lpnmn_0m_0} \int_0^1 r^{n+n_0} \Big\{ & \lambda\gamma_{lp}^1(r) \left[r^2 x_{nn_0}^{(12)(j)}(r) + nn_0 x_{nn_0}^{(13)(j)}(r) \right. \\ & \left. + nl x_{nn_0}^{(14)(j)}(r) \right] + r^2 \dot{\lambda}\gamma_{lp}^1(r) x_{nn_0}^{(15)(j)}(r) \\ & + \mu\gamma_{lp}^1(r) \left[r^2 x_{nn_0}^{(16)(j)}(r) + nn_0 x_{nn_0}^{(17)(j)}(r) + ln_0 x_{nn_0}^{(18)(j)}(r) + lnx_{nn_0}^{(19)(j)}(r) \right] \\ & + \dot{\mu}\gamma_{lp}^1(r) \left[r^2 x_{nn_0}^{(20)(j)}(r) + nn_0 x_{nn_0}^{(21)(j)}(r) \right] \Big\} dr \end{aligned} \tag{50}$$

Definitions of coefficients $x_{nn_0}^{(i)(j)}(r)$ can be found in Appendix C.

4 Final Formulae for Tidal Gravimetric Factors in a Three-Dimensional Inhomogeneous Earth Model

Since the expressions for $F^j(\delta\rho, \delta\mu, \delta\lambda, \delta\tau)$ are determined using equations 15 and 33, the final formulae for the effects of lateral inhomogeneity on gravity can be obtained. These effects can be regarded as gravity changes Δg resulting from lateral inhomogeneity respective to the layered Earth. To facilitate the convenience of using a laterally-inhomogeneous model, the disturbances of rheology parameters $\delta\lambda$ and $\delta\mu$ are replaced with the disturbances of P-wave velocity α, S-wave velocity β, and density γ^1 (Fu & Sun, 2007):

$$\delta\lambda = 2(\lambda + 2\mu)\alpha - 4\mu\beta + \lambda\gamma^1 \tag{51}$$

$$\delta\mu = 2\mu\beta + \mu\gamma^1 \tag{52}$$

In equations 51 and 52, $\alpha = \delta v_p / v_p$, $\beta = \delta v_s / v_s$, and $\gamma^1 = \delta\rho/\rho$. δv_p, δv_s, and $\delta\rho$ are the spherically-asymmetrical increments for P-wave velocity, S-wave velocity, and density, respectively. v_p, v_s, and ρ are mean values of the angle variables with regard to r for P-wave velocity, S-wave velocity, and density, respectively. As shown in Appendix E, with some manipulations, the following is obtained:

$$\Delta g(\theta,\phi)=\sum_{l=0}^{N_e}\sum_{p=-l}^{l}\{\left[\Delta g_{p1}(\theta,\phi)+\Delta g_{s1}(\theta,\phi)+\Delta g_{\rho 1}(\theta,\phi)+\Delta g_{\tau 1}(\theta,\phi)\right]\cos m_0\phi + \left[\Delta g_{p2}(\theta,\phi)+\Delta g_{s2}(\theta,\phi)+\Delta g_{\rho 2}(\theta,\phi)+\Delta g_{\tau 2}(\theta,\phi)\right]\sin m_0\phi\} \tag{53}$$

In equation 53:

$$\Delta g_{p1}(\theta,\phi)=\sum_{n=|l-n_0|}^{l+n_0}\frac{E_{lpn(p\pm m_0)n_0m_0}}{c(n,p\pm m_0)}I(p,p \pm m_0,m_0)Y_n^{p\pm m_0}(\theta,\phi)\int_b^1 2(\lambda+2\mu)y_n(r)\alpha_{lp}(r)dr \tag{54}$$

$$\Delta g_{s1}(\theta,\phi)=\sum_{n=|l-n_0|}^{l+n_0}\frac{E_{lpn(p\pm m_0)n_0m_0}}{c(n,p\pm m_0)}I(p,p \pm m_0,m_0)Y_n^{p\pm m_0}(\theta,\phi)\int_b^1 \{2\mu[z_n(r)-2y_n(r)]\beta_{lp}(r)\}dr \tag{55}$$

$$\Delta g_{\rho 1}(\theta,\phi)=\sum_{n=|l-n_0|}^{l+n_0}\frac{E_{lpn(p\pm m_0)n_0m_0}}{c(n,p\pm m_0)}I(p,p \pm m_0,m_0)Y_n^{p\pm m_0}(\theta,\phi)\int_b^1 \rho(r)\{[q_n^1(r)+\lambda y_n(r)+\mu z_n(r)]\gamma_{lp}^1(r) + q_n^2(r)\gamma_{lp}^2(r)+q_n^3(r)\gamma_{lp}^3(r)\}dr \tag{56}$$

$$\Delta g_{\tau 1}(\theta,\phi)=-\sum_{n=|l-n_0|}^{l+n_0}\frac{E_{lpn(p\pm m_0)n_0m_0}}{c(n,p\pm m_0)}I(p,p \pm m_0,m_0)Y_n^{p\pm m_0}(\theta,\phi)\int_b^1 \gamma_{lp}^1(r)\left[\lambda q_n^4(r)+\dot{\lambda}q_n^5(r)+\mu q_n^6(r)+\dot{\mu}q_n^7(r)\right]dr \tag{57}$$

In equation 54, $\Delta g_{p1}(\theta,\phi)$ is the summation of $\Delta g_{p1}^{+}(\theta,\phi)$ and $\Delta g_{p1}^{-}(\theta,\phi)$, which correspond to replacing "$\pm$" with "$+$" and "$-$", respectively. The same treatment is also applied to equations 55-57. The expressions of $y_n(r)$, $z_n(r)$, and $q_n^i(r), i=1,\ldots,7$ are shown in Appendix E. Besides:

$$I(p, p \pm m, m_0) = \int_0^{2\pi} \cos m_0\phi \begin{cases} \cos p\phi \\ \sin p\phi \end{cases} \begin{cases} \cos(p \pm m_0)\phi \\ \sin(p \pm m_0)\phi \end{cases} d\phi \tag{58}$$

$$Y_n^{p\pm m_0}(\theta, \phi) = P_n^{p\pm m_0}(\cos\theta) \begin{cases} \cos(p \pm m_0)\phi \\ \sin(p \pm m_0)\phi \end{cases} \tag{59}$$

The expressions of $\Delta g_{p2}(\theta, \phi)$, $\Delta g_{s2}(\theta, \phi)$, $\Delta g_{\rho 2}(\theta, \phi)$, and $\Delta g_{\tau 2}(\theta, \phi)$ are the same as those of $\Delta g_{p1}(\theta, \phi)$, $\Delta g_{s1}(\theta, \phi)$, $\Delta g_{\rho 1}(\theta, \phi)$, and $\Delta g_{\tau 1}(\theta, \phi)$, with the only difference being the replacement of $\cos m_0\phi$ in equation 58 with $\sin m_0\phi$. The use of the sine and cosine in the last two terms of equations 58 and 59 is determined as follows:

(1) The second factor in equation 58 is $\cos p\phi$ when $\alpha_{lp}(r)$, $\beta_{lp}(r)$, and $\gamma_{lp}^1(r)$ are the coefficients of $\cos p\phi$, whereas the second factor is $\sin p\phi$ when $\alpha_{lp}(r)$, $\beta_{lp}(r)$, and $\gamma_{lp}^1(r)$ are the coefficients of $\sin p\phi$;

(2) The third factor in equation 58 is $\cos(p \pm m_0)\phi$ when the first two factors in equation 58 are both sines or both cosines, otherwise the third factor is $\sin(p \pm m_0)\phi$;

(3) When the third factor in equation 58 is $\cos(p \pm m_0)\phi$, equation 59 is written as:

$$Y_n^{p\pm m_0}(\theta, \phi) = P_n^{p\pm m_0}(\cos\theta) \cos(p \pm m_0)\phi$$

When the third factor in equation 58 is $\sin(p \pm m_0)\phi$, equation 59 is written as:

$$Y_n^{p\pm m_0}(\theta, \phi) = P_n^{p\pm m_0}(\cos\theta) \sin(p \pm m_0)\phi$$

Finally, the change of gravimetric factor is obtained:

$$\delta_1(\theta, \phi) = \frac{1}{\delta_{n_0} P_{n_0}^{m_0}(\cos\theta)} \sum_{l=0}^{N_e} \sum_{p=-l}^{l} \{\Delta g_1(\theta, \phi) \cos m_0\phi + \Delta g_2(\theta, \phi) \sin m_0\phi\} \tag{60}$$

In equation, 60, $\Delta g_1(\theta, \phi)$ is the summation of $\Delta g_{p1}(\theta, \phi)$, $\Delta g_{s1}(\theta, \phi)$, $\Delta g_{\rho 1}(\theta, \phi)$, and $\Delta g_{\tau 1}(\theta, \phi)$. $\Delta g_2(\theta, \phi)$ is the summation of $\Delta g_{p2}(\theta, \phi)$, $\Delta g_{s2}(\theta, \phi)$, $\Delta g_{\rho 2}(\theta, \phi)$, and $\Delta g_{\tau 2}(\theta, \phi)$. The gravimetric factor is written as:

$$\delta_{n_0} = 1 - \frac{n_0 + 1}{n_0} k_{n_0} + \frac{2}{n_0} h_{n_0} \tag{61}$$

In equation 61, h_{n_0} and k_{n_0} are tidal Love numbers of degree n_0, describing the variations in vertical displacement and gravitational potential at the surface, respectively.

5 Validation of the Three-Dimensional Tidal Theory

This section details the results of the numerical test and the verification of the three-dimensional tidal theory through comparison of the results with those of previous studies. The

test algorithm was first proposed by Molodenskii & Kramer (1980) who constructed a simple ocean-land model, which is then used for evaluating the effects of P-wave and S-wave velocity disturbances based on an ocean function. The ocean function is a delta function with values of 1 and 0 for under the ocean and under the continent, respectively. Balmino et al. (1973) presented the 8-degree spherical harmonic expanded form of the ocean function. The velocities of P-wave and S-wave under the ocean in the ocean-land model are 5% lower than those under the continent. The ocean-land model is suitable for the numerical test since its values under the continent and ocean are positive and negative, respectively. The signs of the results of the test with the ocean-land model conducted in the present study are opposite to those of Molodenskii & Kramer (1980). The treatment by Molodenskii & Kramer (1980) on the ocean function was contrary to that of the current study as they regarded the values under the ocean and under the continent as 0 and 1, respectively. To facilitate a comparison of the results of the present study with those of Molodenskii & Kramer (1980), it is assumed that the value under the ocean is 5% higher than that under the continent so as to construct a new ocean-land model (Figure 1).

Once the Earth model is identified, the effects of lateral inhomogeneity on semidiurnal gravimetric factors can be computed with the use of equation 60. It should be noted that the polar effect is observable in the results. Because the denominator approaches 0 with an increase in latitude, the numerical error at polar regions may be amplified. This error has little influence on middle-low latitude regions which is the focus of the current study and is hard to avoid. Therefore, the current study shows the results from 75 °S to 75 °N only.

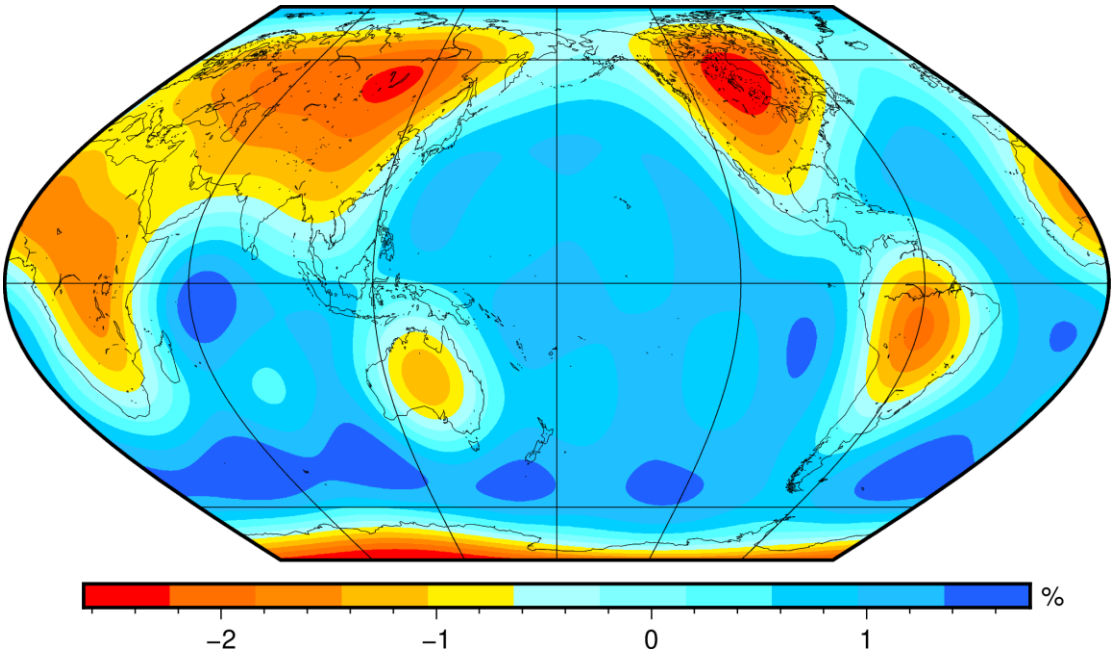

Figure 1. The ocean-land model used for the numerical test in the current study. The model is determined with the help of an 8-degree spherical harmonic expanded ocean function (Balmino et al., 1973). The value under the ocean is 5% higher than that under the continent to facilitate a comparison with the results of Molodenskii & Kramer (1980).

Figure 2a illustrates the effects of perturbation of P-wave velocity on semidiurnal gravimetric factors calculated for the ocean-land model. The patterns are principally consistent with the ocean-land model as the value under the ocean is distinct from that under the continent. Although the actual values determined in the present study (−1.2% to 1.1%) are approximately close to those (−1.1% to 0.8%) of Molodenskii & Kramer (1980), discrepancies exist for some regions. These discrepancies arise from the fact that the two studies adopt different spherically-symmetrical models for the computation of one-dimensional solutions and auxiliary solutions. Molodenskii & Kramer (1980) adopted the model 508 of Gilbert & Dziewonski (1975), whereas the current study adopts the preliminary reference Earth model (PREM, Dziewonski & Anderson, 1981). The accuracy of PREM exceeds that of model 508, resulting in the distributions generated by the current study being closer to the ocean-land model compared to those of Molodenskii & Kramer (1980).

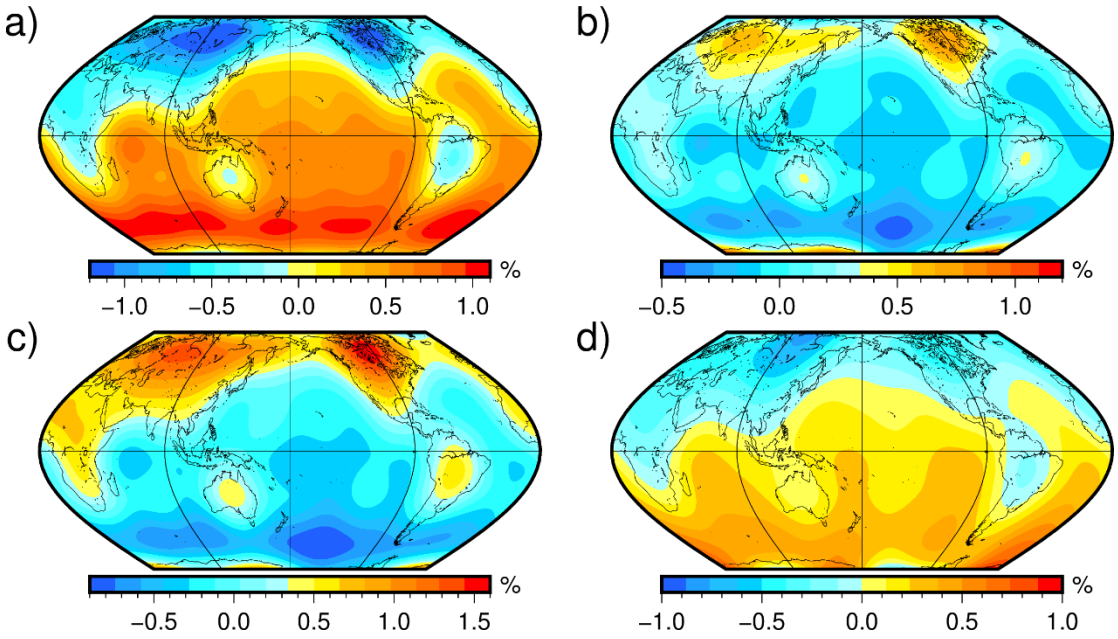

Figure 2. Changes in semidiurnal gravimetric factors calculated for the ocean-land model. Effects of a) the lateral inhomogeneity of P-wave velocity, b) the lateral inhomogeneity of S-wave velocity, c) the lateral inhomogeneity of density, and d) non-hydrostatic pre-stress are illustrated. All patterns of the four subfigures are consistent with the ocean-land model to some extent. The value under the ocean is generally positive whereas that under the continent is generally negative in a) and d), and vice versa in b) and c). The four kinds of effects are almost at the same level.

Figure 2b-2d illustrate the effects of lateral inhomogeneity of S-wave velocity, density, and non-hydrostatic pre-stress on semidiurnal gravimetric factors. The patterns of these results are also consistent with the ocean-land model. The effects of S-wave velocity disturbance, density disturbance, and non-hydrostatic pre-stress range from −0.5% to 1.2%, −0.9% to 1.6%, and −1.0% to 1.0%, respectively. It should be noted that the disturbances of P-wave velocity, S-wave velocity, and density in a real Earth model inevitably differ, and therefore should not share

the same model. In particular, the density disturbance is lower than that of seismic wave velocity by a factor of approximately 0.2 to 0.5 (Karato, 1993). As a result, the ocean-land model can be applied in a numerical test but not for a real situation. The test results demonstrate that when the models are the same, the effects of density disturbance and non-hydrostatic pre-stress on semidiurnal gravimetric factors are at the same level as those of seismic wave velocity disturbance. The effects of non-hydrostatic pre-stress can therefore not be ignored.

The effects of P-wave velocity disturbance for the upper mantle (from surface to a depth of 331 km) and the lower mantle (from a depth of 331 km to a depth of 2,891 km) are computed (Figure 3) for comparison with the results of Fu & Sun (2007). The results of the present study are generally consistent with those of Fu & Sun (2007) except for handful of regions. The discrepancies in these regions may be attributed to two factors: 1) Fu & Sun (2007) directly integrated the product of three Legendre functions to compute $E_{lpnmn_0m_0}$, whereas the results of the current study are more accurate as $E_{lpnmn_0m_0}$ is computed using the analytical solution proposed by Fu & Sun (2008); 2) the ocean function used for constructing the ocean-land model has been corrected once (Balmino et al., 1973), and while Fu & Sun (2007) used the uncorrected function, the current study uses the corrected function, resulting in differences at high-latitude regions. In regards to the distribution of δ_1, the results of the present study reflect the distinctions between ocean and continent, and show a better consistency with the ocean-land model compared to the results of Fu & Sun (2007). Therefore, the three-dimensional tidal theory presented in the current study is correct and valid.

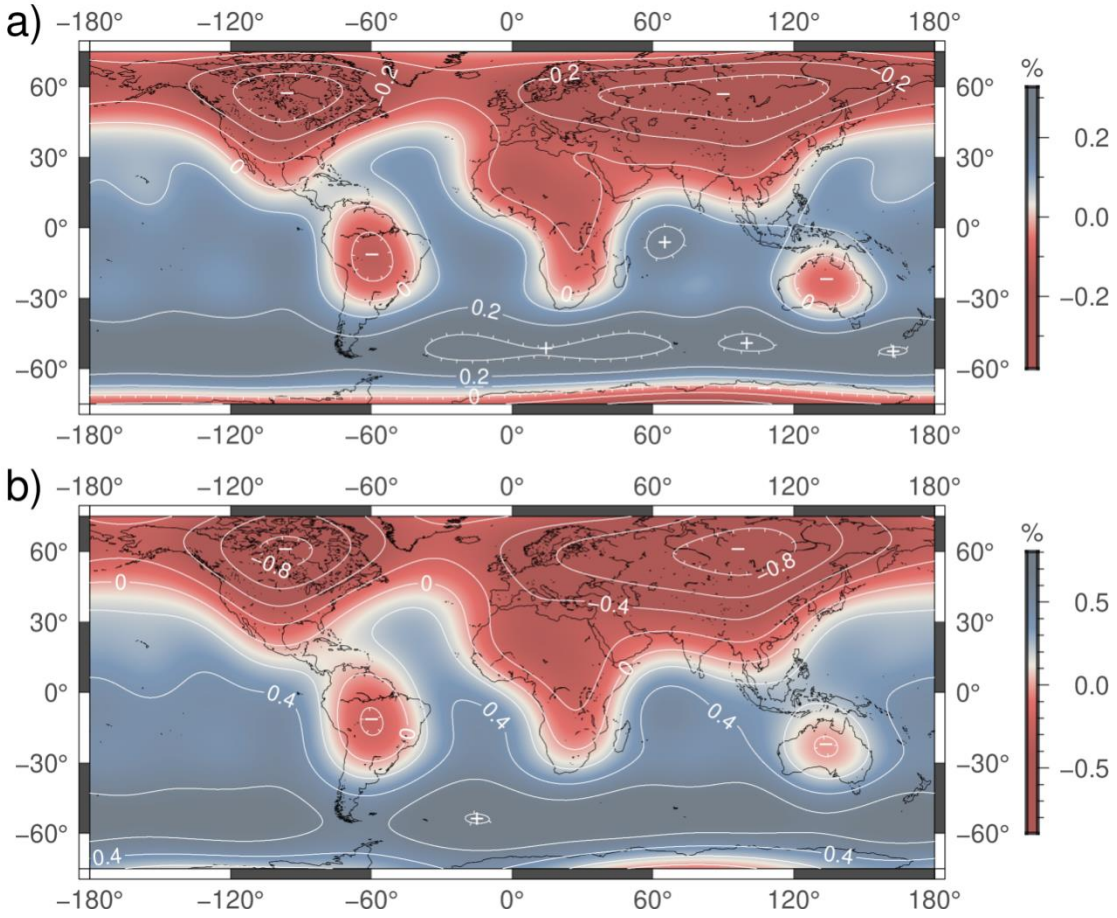

Figure 3. Comparison of the effects of P-wave velocity disturbance on semidiurnal gravimetric factors for a) the upper mantle (from surface to a depth of 331 km) and b) the lower mantle (from a depth of 331 km to a depth of 2,891 km). While the magnitudes of the present study are almost the same as those of Fu & Sun (2007), the distributions of the current study are more consistent with the ocean-land model.

6 Global Distribution of the Theoretical Semidiurnal Tidal Gravimetric Factor

While the ocean-land model can distinguish between ocean and continent, it is unable to truly reflect the lateral inhomogeneity of the Earth. The current study adopts the three-dimensional Earth model GyPSuM (Simmons et al., 2010) to determine the real effects of lateral inhomogeneity. The model is developed through simultaneous inversion of seismic wave travel times and geodynamic observations. GyPSuM incorporates models of P-wave velocity, S-wave velocity, and density, which can be downloaded from the Incorporated Research Institutions for Seismology (IRIS) website (http://ds.iris.edu/ds/products/emc-Earthmodels/, Trabant et al., 2012). As mentioned above, the current study also requires the three-dimensional gravity model and its derivatives for computing, which can be determined by integrating the density model.

Figure 4 shows the changes in the semidiurnal gravimetric factors calculated using the real three-dimensional P-wave model and S-wave model, which range from −0.45% to 0.39% and −0.26% to 0.34%, respectively. Both changes are less than those indicated in the results of the ocean-land model. The deviation is attributed to the fact that the real models generally have smaller values in deep mantle compared to the ocean-land model. Figures 4a and 4b show similar

patterns with generally opposite signs, and this feature is also evident in the results for the ocean-land model. While not as obvious as indicated in the results of the ocean-land model, the results of real three-dimensional models are similarly consistent with the distributions of land and continent. The effects of P-wave velocity disturbance are generally positive and negative under continent and under ocean, respectively, whereas S-wave velocity disturbance has the opposite effects. Only a few regions, including southeastern Asia, western North America, and eastern Africa, show anomalies, indicating that although the ocean-land model is simple, it is at least partly plausible.

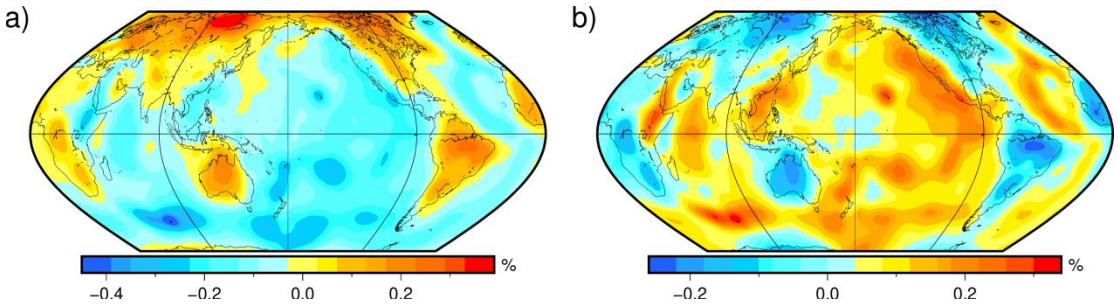

Figure 4. Changes in the semidiurnal gravimetric factor resulting from a) the perturbation of P-wave velocity and b) the perturbation of S-wave velocity. Results in a) are calculated by the real three-dimensional P-wave model and in b) are calculated by the real three-dimensional S-wave model. The range of changes indicated in these results are approximately a third or half of those indicated by the results of the ocean-land model, suggesting that the effects of lateral inhomogeneity are overestimated by the ocean-land model. The patterns of the two models are similar and the signs of the models are in general opposite.

Figure 5 shows the changes to the semidiurnal gravimetric factors resulting from density disturbance and non-hydrostatic pre-stress calculated by the real three-dimensional density model in GyPSuM, with the ranges of changes being −0.12% to 0.09% and −0.04% to 0.05%, respectively. The changes due to these two kinds of effects as calculated by the real three-dimensional density model are notably smaller compared to those calculated by the real three-dimensional seismic wave models. The numerical test demonstrates that the four kinds of effects are at similar levels, which can be attributed to the real density model being smaller than the real seismic wave models. Figure 5a and Figure 4b show similar patterns, consistent with behavior reported by Fu & Sun (2007). Analogous to those calculated by seismic wave models, the changes in the semidiurnal gravimetric factors calculated by the density model are also consistent with the distributions of ocean and continent.

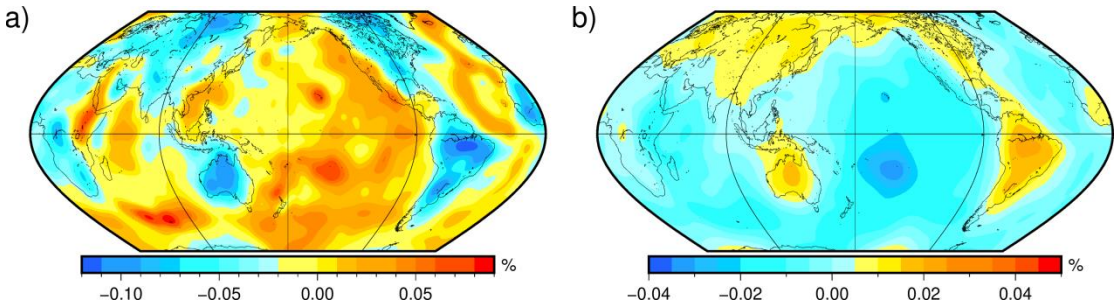

Figure 5. Changes in the semidiurnal gravimetric factor resulting from a) density disturbance and b) non-hydrostatic pre-stress calculated by the real three-dimensional density model GyPSuM. Results illustrated in a) are determined by the density model, gravity model, and its derivative. The influences of the density model are much larger than those of the other models, and as a result, it can be concluded for convenience that the changes result from density disturbance.

The four kinds of effects as shown in Figures 4 and 5 can then be summed to obtain the total changes in semidiurnal gravimetric factor resulting from lateral inhomogeneity (Figure 6). The changes range from −0.15% to 0.09%, similar to those calculated by the density model and smaller than those calculated by the seismic wave models. Density disturbance and non-hydrostatic pre-stress are the major contributors to total changes, although their effects are smaller than those of P-wave velocity disturbance and S-wave velocity disturbance. This is because the effects of the two kinds of seismic wave velocity disturbance offset each other as while they have similar distributions with opposite signs. Consequently, density disturbance and non-hydrostatic pre-stress have a significant influence on tidal gravity and are not negligible. The total changes are negative in the central Pacific, central Eurasia, Australia, South America, North America, and Africa, while they are positive in other regions. The largest negative change is in western Africa, whereas the largest positive change is in southeastern Asia.

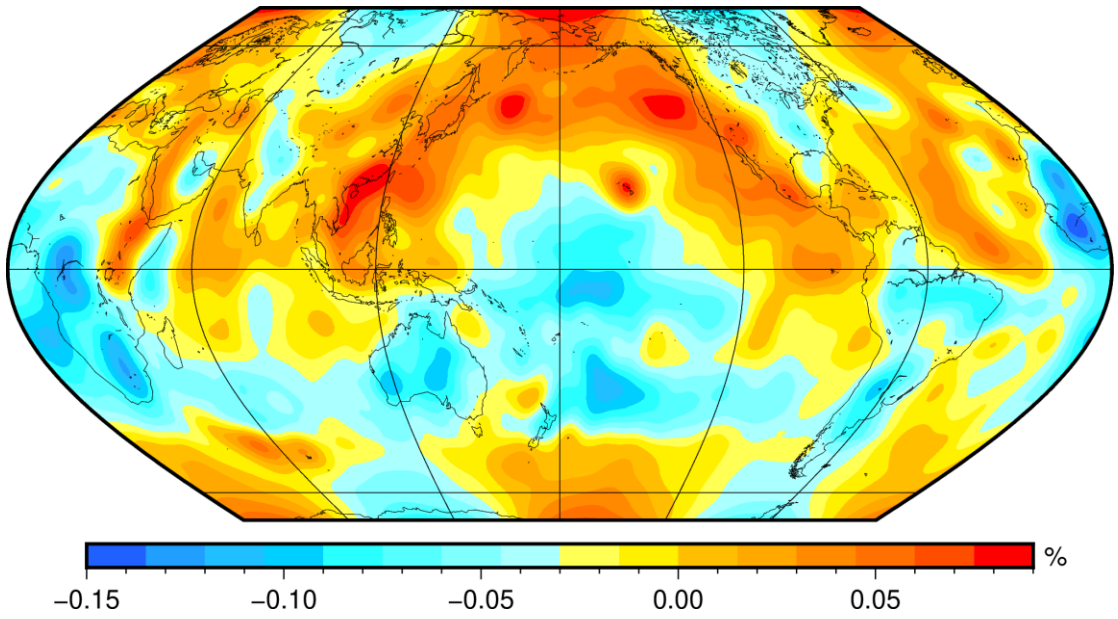

Figure 6. Total changes in the semidiurnal gravimetric factors as calculated by the real three-dimensional Earth model GyPSuM (Simmons et al., 2010) respective to the spherically-symmetrical Earth model. The results are identical to the summation of Figures 4a, 4b, 5a, and 5b.

In light of equation 60, the results shown in Figure 6 can be regarded as corrections to theoretical tidal gravimetric factors calculated for spherically-symmetrical models. Therefore, a comparison of the theoretical factors to measurements after correction using the results in Figure 6 can be used to validate the tidal theory. The M2 tidal gravimetric factor measurements (Boy et al., 2003; Sun et al., 2019) of 14 superconducting gravimeters located at Lhasa, Lijiang, Wuhan, Boulder, Cantley, Canberra, Esashi, Matsushiro, Membach, Metsahovi, Potsdam, Strasbourg, Syowa, and Vienna are collected (Figure 7). The corresponding theoretical values are calculated using the WPARICET program which can be downloaded from the International Center for Earth Tide (ICET) website (https://www.astro.oma.be/en/). Ocean tidal loading is estimated using the CSR3.0 model (Eanes & Bettadpur, 1996). Table 1 shows the detailed data.

Table 1. Information for Superconducting Gravimeter Stations and M2 Gravimetric Factor Values

Number	Location	Latitude (°)	Longitude (°)	Altitude (m)	Measurement	Uncorrected theoretical value	Corrected theoretical value
01	Lhasa	29.645	91.035	3632	1.16289	1.15952	1.15956
02	Lijiang	26.896	100.232	2435	1.16575	1.16206	1.16213
03	Wuhan	30.516	114.490	89	1.17159	1.17076	1.17109
04	Boulder	40.131	245.767	1682	1.15944	1.14451	1.14496
05	Cantley	45.585	284.193	269	1.20349	1.20376	1.20341
06	Canberra	-35.321	149.008	762	1.18585	1.18284	1.18255
07	Esashi	39.151	141.332	434	1.19300	1.18753	1.18809
08	Matsushiro	36.544	138.203	451	1.19098	1.19228	1.19281
09	Membach	50.609	6.007	250	1.18824	1.18818	1.18820
10	Metsahovi	60.217	24.396	56	1.18187	1.15810	1.15865
11	Potsdam	52.381	13.068	81	1.18585	1.18431	1.18522
12	Strasbourg	48.622	7.684	180	1.18710	1.18576	1.18565
13	Syowa	-69.007	39.595	24	1.40054	1.36340	1.36447
14	Vienna	48.249	16.358	80	1.18170	1.18120	1.18141

A correction function is defined for visually displaying the correction effects:

$$F_{cor} = \frac{|\delta_{the1} - \delta_{mea}| - |\delta_{the2} - \delta_{mea}|}{|\delta_{the1} - \delta_{mea}|} \tag{62}$$

In equation 62, the double vertical lines indicate the absolute value, δ_{mea} is the measurement, δ_{the1} is the uncorrected theoretical value, δ_{the2} is the corrected theoretical value, namely, $\delta_{the2} = (1 + \delta_1)\delta_{the1}$. F_{cor} indicates the correction effect, it is positive if the theoretical value is close to the measurement after correction, and negative otherwise, and F_{cor} is equal to 1 if the corrected theoretical value equals the measurement. Figure 7 shows the correction effects. The theoretical values at 11 of 14 superconducting gravimeters are close to the measurements after correction, with those of stations 06, 08, and 12 deviating from the measurements after correction. Station 05 showed the best correction effect with the F_{cor} exceeding 70%. Although station 07 is situated close to station 08, the correction effects for these two stations vary widely. This discrepancy can be attributed to the difference in the theoretical values for the two stations, with the theoretical value exceeding the measurement for station 08, whereas the opposite is true for station 07, and there being small positive changes in the gravimetric factors for both stations. As a result, the theoretical value of station 07 is closer to the measurement after correction whereas the theoretical value for station 08 deviates from the measurement after correction. The correction functions at four of five stations in western Europe (09, 10, 11, and 14) are positive with an average F_{cor} exceeding 25%. The correction functions of three stations in eastern Asia (01, 02, and 03), two stations in North America (04 and 05), and one station in a high latitude region (13) are positive. In summary, the comparison between calculated results and measurements reveals a relatively good correlation, indicating that the expressions presented in the current study are correct.

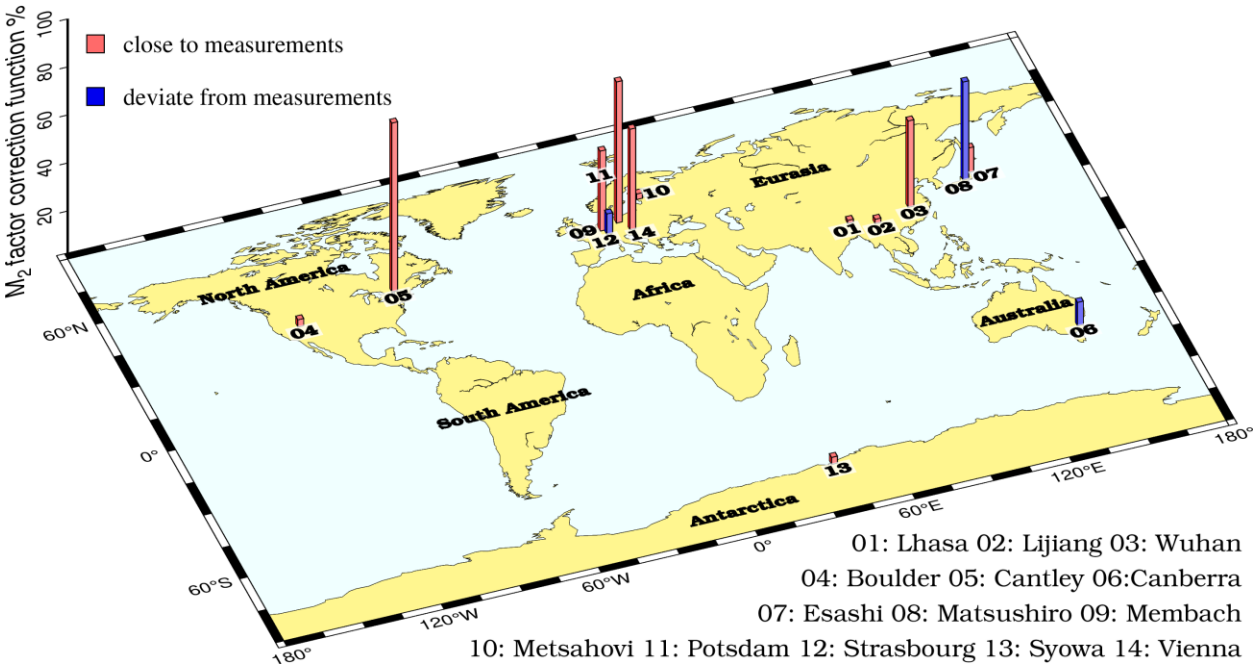

Figure 7. Correction functions of the M2 components of tidal gravimetric factors. Red columns represent the theoretical values close to measurements after considering the lateral inhomogeneity of the Earth. Blue columns represent the theoretical values that deviate from measurements after considering the lateral inhomogeneity of the Earth. The solutions are expressed in percent. Station 5 shows the best correction effect whereas station 08 shows the worst.

7 Conclusion

Although Molodenskiy (1980), Fu & Sun (2007), and others researched the effects of laterally-inhomogeneous seismic wave velocity and density on tidal gravity, very few of these studies considered the contribution of non-hydrostatic pre-stress. Within tidal theory, non-hydrostatic pre-stress results from the transition from a spherically-symmetrical model to a spherically-asymmetrical model when introducing asymmetric density increments. These density increments are smaller than increments in the rheology parameters. Consequently, the effects of non-hydrostatic pre-stress have been directly neglected in previous studies. The current study presents expressions for the effects of non-hydrostatic pre-stress on tidal gravimetric factors. The present study develops the tidal theory for a laterally-inhomogeneous Earth model and performs a numerical test. The results of the present study based on a real Earth model suggest that although the effects of non-hydrostatic pre-stress are less than those of seismic wave velocity disturbance, the contribution of non-hydrostatic pre-stress to the final results is significant and therefore cannot be ignored.

The present study calculates changes to semidiurnal tidal gravimetric factors using the simple ocean-land model (Molodenskii & Kramer, 1980) and the real three-dimensional Earth model GyPSuM (Simmons et al., 2010). The distribution patterns of changes shown in the two sets of theoretical results are consistent to some extent with the distribution of ocean and continent. The results calculated by the ocean-land model indicate that the effects of seismic wave velocity disturbance, density disturbance, and non-hydrostatic pre-stress are at the same level when the same model is used. Within the results of GyPSuM, the changes to the gravimetric factor resulting from the lateral inhomogeneity of P-wave velocity, S-wave velocity, density, and non-hydrostatic pre-stress are in the ranges of −0.45% to 0.39%, −0.26% to 0.34%, −0.12% to 0.09%, and −0.04% to 0.05%, respectively. When adding the four kinds of contributions, the total changes to the gravimetric factor are obtained. The total changes are negative in the central Pacific, central Eurasia, Australia, North America, South America, and Africa, and positive in other regions. The largest negative change is in western Africa, whereas the largest positive change is in southeastern Asia, and the changes vary from −0.16% to 0.09% compared with the values of a layered Earth model. The effects of P-wave velocity disturbance and S-wave velocity disturbance offset each other as while they have similar distributions with opposite signs. Consequently, density disturbance and non-hydrostatic pre-stress have a major influence on tidal gravity. The theoretical results demonstrate that the effects of non-hydrostatic pre-stress on tidal gravity are not negligible.

The results presented by the current study can be regarded as corrections to theoretical tidal gravimetric factors calculated for spherically-symmetrical models. M2 tidal gravimetric factor measurements of 14 superconducting gravimeters distributed globally (Boy et al., 2003; Sun et al., 2019) are collected and compared to the theoretical results to verify the expressions presented in the current study. The results of this verification exercise show that the theoretical values at 11 of 14 stations are close to measurements after correction, with theoretical values of only 3 of 14 stations deviating from measurements after correction. The results indicate that the expressions presented in the current study for calculating the effects of lateral inhomogeneity on tidal gravimetric factors are valid.

Acknowledgments, Samples, and Data

The authors received funding from the National Natural Science Foundation of China (41 874003), the National Key R&D Program of China (2018YFC1503704), and the Special Fund of the Institute of Earthquake Forecasting, China Earthquake Administration (2020IEF0708).

Data Availability Statement

The real three-dimensional Earth model GyPSuM can be found on IRIS website (see http://ds.iris.edu/ds/products/emc-Earthmodels/). The WPARICET program used for calculating theoretical gravimetric factors can be found on ICET website (see https://www.astro.oma.be/en/). Measurements of superconducting gravimeters are published data and are available as referenced in Boy et al. (2003) and Sun et al. (2019).

Appendix A: Algorithms for Coefficients $y_i(r)$

Determining coefficients $y_i(r), i = 1, \ldots, 6$ is the key process to obtain the solutions of Love numbers and Green's functions. The explicit expressions for calculating $y_i(r)$ have been presented by many researchers (Longman, 1963; Sun & Okubo, 1993). Although deviations of definitions and treatments may exist in different papers, the final results are basically the same. Here the expressions proposed by Longman (1963) are addressed. According to definition, $y_i(r)$ satisfies:

$$\dot{y}_1(r) = -\frac{2\lambda}{\lambda+2\mu}\frac{y_1(r)}{r} + \frac{y_2(r)}{\lambda+2\mu} + n(n+1)\frac{\lambda}{\lambda+2\mu}\frac{y_3(r)}{r} \tag{A1}$$

$$\dot{y}_2(r) = \left[-4C\rho gr + \frac{4\mu(3\lambda+2\mu)}{\lambda+2\mu}\right]\frac{y_1(r)}{r^2} - \frac{4\mu}{\lambda+2\mu}\frac{y_2(r)}{r} + n(n+1)\left[C\rho gr - \frac{2\mu(3\lambda+2\mu)}{\lambda+2\mu}\right]\frac{y_3(r)}{r^2} + n(n+1)\frac{y_4(r)}{r} - C\rho y_6(r) \tag{A2}$$

$$\dot{y}_3(r) = -\frac{y_1(r)}{r} + \frac{y_3(r)}{r} + \frac{y_4(r)}{\mu} \tag{A3}$$

$$\dot{y}_4(r) = \left[C\rho gr - \frac{2\mu(3\lambda+2\mu)}{\lambda+2\mu}\right]\frac{y_1(r)}{r^2} - \frac{\lambda}{\lambda+2\mu}\frac{y_2(r)}{r} + \frac{2\mu}{\lambda+2\mu}[\lambda(2n^2+2n-1) + 2\mu(2n^2+2n-1)]\frac{y_3(r)}{r^2} - 3\frac{y_4(r)}{r} - C\rho\frac{y_5(r)}{r} \tag{A4}$$

$$\dot{y}_5(r) = B\rho y_1(r) + y_6(r) \tag{A5}$$

$$\dot{y}_6(r) = -n(n+1)B\rho\frac{y_3(r)}{r} + n(n+1)B\rho\frac{y_5(r)}{r^2} - 2\frac{y_6(r)}{r}$$

(A6)

In equations A1-A6,

$$\begin{cases} B = 4\pi G\rho_0 a/g_0 \\ C = \rho_0 g_0 a/\lambda_0 \end{cases}$$

(A7)

G is Newton's gravitational constant, ρ_0 and λ_0 are density and rheology parameter at the center of Earth, a and g_0 are radius and gravity on the surface of Earth. $y_i(r)$ can be determined by integrating the differential equations from core-mantle boundary to surface by Runge-Kutta method, with the help of following boundary conditions,

$$\begin{cases} y_2(a) = 0 \\ y_4(a) = 0 \\ y_6(a) + (n+1)y_5(a) = 2n+1 \end{cases}$$

(A8)

Appendix B: Treatment of $A_{lpnmn_0m_0}$

Equation 39 can be written as:

$$A_{lpnmn_0m_0} = \iint Y_l^p(\theta,\phi)Y_n^m(\theta,\phi)Y_{n_0}^{m_0}(\theta,\phi)dS = E_{lpnmn_0m_0}I(p,m,m_0)$$

(B1)

$$E_{lpnmn_0m_0} = \int_{-\frac{\pi}{2}}^{\frac{\pi}{2}} P_l^p(\cos\theta)P_n^m(\cos\theta)P_{n_0}^{m_0}(\cos\theta)d\theta$$

(B2)

$$I(p,m,m_0) = \int_0^{2\pi} \begin{cases}\cos p\phi \\ \sin p\phi\end{cases} \begin{cases}\cos m\phi \\ \sin m\phi\end{cases} \begin{cases}\cos m_0\phi \\ \sin m_0\phi\end{cases} d\phi$$

(B3)

In light of Fu & Sun (2008), the normalized form of $E_{lpnmn_0m_0}$ is

$$\bar{E}_{lpnmn_0m_0} = 4\sqrt{2}(-1)^p(2l+1)^{1/2}(2n+1)^{1/2}(2n_0+1)^{1/2}\begin{pmatrix} l & n & n_0 \\ -p & m & m_0 \end{pmatrix}\begin{pmatrix} l & n & n_0 \\ 0 & 0 & 0 \end{pmatrix}$$

(B4)

The value of $\bar{E}_{lpnmn_0m_0}$ need to divide $\sqrt{2}$ if each of p, m, and m_0 equals 0. The Wigner 3j symbol in equation B4 is defined as following.

$$\begin{pmatrix} a & b & c \\ \alpha & \beta & \gamma \end{pmatrix} = (-1)^{a-b-\gamma}\left[\frac{(a+b-c)!\,(a-b+c)!\,(-a+b+c)!}{(a+b+c+1)!}\right]^{\frac{1}{2}}[(a+\alpha)!\,(a-\alpha)!\,(b+\beta)!\,(b-\beta)!\,(c+\gamma)!\,(c-\gamma)!]^{\frac{1}{2}}\sum_{k}(-1)^{k}[k!\,(a+b-c-k)!\,(a-\alpha-k)!\,(b+\beta-k)!\,(c-a-\beta-k)!\,(c-b+\alpha+k)!]^{-1}$$

(B5)

The range of k is limited to make sure that all factorials in the denominator are non-negative.

As for $I(p,m,m_0)$,

$$\int_0^{2\pi}\sin m_1\phi\cos m_2\phi\cos m_3\phi\,d\phi = 0$$

(B6)

$$\int_0^{2\pi}\sin m_1\phi\sin m_2\phi\sin m_3\phi\,d\phi = 0$$

(B7)

$$\int_0^{2\pi}\cos m_1\phi\cos m_2\phi\cos m_3\phi\,d\phi = \frac{\pi}{2}\left[\delta_{m_1+m_2,m_3}+\delta_{m_2+m_3,m_1}+\delta_{m_1+m_3,m_2}+\delta_{m_1+m_2,-m_3}\right]$$

(B8)

$$\int_0^{2\pi}\sin m_1\phi\cos m_2\phi\sin m_3\phi\,d\phi = \frac{\pi}{2}\left[\delta_{m_2+m_3,m_1}-\delta_{m_1+m_3,m_2}+\delta_{m_1+m_2,m_3}-\delta_{m_1+m_2,-m_3}\right]$$

(B9)

Appendix C: Expressions of $x_{nn_0}^{(i)(j)}(r)$

In equations 36 and 37,

$$x_{nn_0}^{(1)(j)}(r) = r^2\left[\dot{y}_1^0(r)+\frac{2}{r}y_1^0(r)-\frac{n_0(n_0+1)}{r}y_3^0(r)\right]\cdot\left[\dot{y}_1^j(r)+\frac{2}{r}y_1^j(r)-\frac{n(n+1)}{r}y_3^j(r)\right]$$

(C1)

$$x_{nn_0}^{(2)(j)}(r) = 2r^2\left\{r^2\dot{H}_n^j\dot{H}_{n_0} + r\dot{H}_n^j H_{n_0} + rH_n^j\dot{H}_{n_0} + nr\dot{H}_{n_0}\left(H_n^j + \frac{\dot{T}_n^j}{r}\right) + n_0 r\dot{H}_n^j\left(H_{n_0} + \frac{\dot{T}_{n_0}}{r}\right) + \frac{n(n-1)}{r}\dot{H}_{n_0}T_n^j + \frac{n_0(n_0-1)}{r}\dot{H}_n^j T_{n_0} + 3H_n^j H_{n_0} + nH_{n_0}\left(H_n^j + \frac{\dot{T}_n^j}{r}\right) + n_0 H_n^j\left(H_{n_0} + \frac{\dot{T}_{n_0}}{r}\right) + \frac{nn_0}{2}\left(H_{n_0} + \frac{\dot{T}_{n_0}}{r}\right)\left(H_n^j + \frac{\dot{T}_n^j}{r}\right)\right\}$$

(C2)

$$x_{nn_0}^{(3)(j)}(r) = \left\{r^2\left(H_{n_0} + \frac{\dot{T}_{n_0}}{r}\right)\left(H_n^j + \frac{\dot{T}_n^j}{r}\right) + 2(n-1)T_n^j\left(H_{n_0} + \frac{\dot{T}_{n_0}}{r}\right) + 2(n_0-1)T_{n_0}\left(H_n^j + \frac{\dot{T}_n^j}{r}\right)\right\}$$

(C3)

$$x_{nn_0}^{(4)(j)}(r) = \frac{2}{r^2}T_n^j T_{n_0}$$

(C4)

In equations C2-C4:

$$H_n^j = \frac{y_1^j(r)}{r^{n+1}} - \frac{ny_3^j(r)}{r^{n+1}};\ T_n^j = \frac{y_3^j(r)}{r^{n-1}}$$

$$H_{n_0}(r) = \frac{y_1^0(r)}{r^{n_0+1}} - \frac{n_0 y_3^0(r)}{r^{n_0+1}};\ T_{n_0}(r) = \frac{y_3^0(r)}{r^{n_0-1}}$$

(C5)

In equation 38,

$$x_{nn_0}^{(5)(j)}(r) = r^{n+n_0+2}\left[h_{n_0}^0(r)h_n^1(r) + h_n^j(r)h_{n_0}^4(r) + g(r)h_n^j(r)h_{n_0}^2(r)\right] - g(r)r^2 y_1^j(r)D_{n_0}(r)$$

(C6)

$$x_{nn_0}^{(6)(j)}(r) = r^{n+n_0}\left[t_{n_0}^0(r)t_n^1(r) + t_n^j(r)t_{n_0}^4(r) + g(r)t_n^j(r)t_{n_0}^2(r)\right]$$

(C7)

$$x_{nn_0}^{(7)(j)}(r) = r^{n+n_0+2}g(r)h_n^j(r)h_{n_0}^2(r) - g(r)r^2 y_1^j(r)D_{n_0}(r)$$

(C8)

$$x_{nn_0}^{(8)(j)}(r) = r^{n+1}g(r)h_n^j(r)y_1^0(r)$$

(C9)

$$x_{nn_0}^{(9)(j)}(r) = r^{n+n_0}g(r)t_n^j(r)t_{n_0}^2(r)$$

(C10)

$$x_{nn_0}^{(10)(j)}(r) = r^n g(r) t_n^j(r) y_1^0(r)$$

(C11)

$$x_{nn_0}^{(11)(j)}(r) = r^{n+2} \dot{g}(r) h_n^j(r) y_1^0(r)$$

(C12)

where,

$$D_{n_0}(r) = \dot{y}_1^0(r) + \frac{2}{r} y_1^0(r) - \frac{n_0(n_0+1)}{r} y_3^0(r)$$

(C13)

$$h_{n_0}^0(r) = \frac{y_1^0(r)}{r^{n_0}} - \frac{n_0 y_3^0(r)}{r^{n_0}};\ t_{n_0}^0(r) = \frac{y_3^0(r)}{r^{n_0-1}}$$

(C14)

$$h_n^j(r) = \frac{y_1^j(r)}{r^n} - \frac{n y_3^j(r)}{r^n};\ t_n^j(r) = \frac{y_3^j(r)}{r^{n-1}}$$

(C15)

$$h_n^1(r) = \frac{\dot{y}_5^j(r)}{r^n} - \frac{n y_5^j(r)}{r^{n+1}};\ t_n^1(r) = \frac{y_5^j(r)}{r^n}$$

(C16)

$$h_{n_0}^2(r) = \frac{\dot{y}_1^0(r)}{r^{n_0}} - \frac{n_0 y_1^0(r)}{r^{n_0+1}};\ t_{n_0}^2(r) = \frac{y_1^0(r)}{r^{n_0}}$$

(C17)

$$h_{n_0}^4(r) = \frac{\dot{y}_5^0(r)}{r^{n_0}} - \frac{n_0 y_5^0(r)}{r^{n_0+1}};\ t_{n_0}^4(r) = \frac{y_5^0(r)}{r^{n_0}}$$

(C18)

In equation 50,

$$x_{nn_0}^{(12)(j)}(r) = \frac{H_n^j \dot{D}_{n_0}}{r^{n_0-1}} + T_n^j \left[\frac{n \dot{D}_{n_0}}{r^{n_0+1}} - \frac{n(n_0+l) D_{n_0}}{r^{n_0+2}} \right]$$

(C19)

$$x_{nn_0}^{(13)(j)}(r) = \frac{T_n^j D_{n_0}}{r^{n_0}}$$

(C20)

$$x_{nn_0}^{(14)(j)}(r) = \frac{T_n^j D_{n_0}}{r^{n_0}}$$

(C21)

$$x_{nn_0}^{(15)(j)}(r) = \frac{H_n^j D_{n_0}}{r^{n_0-1}} + \frac{nT_n^j D_{n_0}}{r^{n_0+1}}$$

(C22)

$$\begin{aligned} x_{nn_0}^{(16)(j)}(r) = H_n^j \Bigg[& 2r^2\ddot{H}_{n_0} + r\left(8\dot{H}_{n_0} + 4n_0\dot{H}_{n_0}\right) - n_0(l-n_0-5)H_{n_0} + 2n_0\ddot{T}_{n_0} \\ & - \frac{n_0(l-3n_0+1)\dot{T}_{n_0}}{r} - \frac{2ln_0(n_0-1)T_{n_0}}{r^2} \Bigg] \\ & + T_n^j \Bigg[2n\ddot{H}_{n_0} + \frac{8n\dot{H}_{n_0} + 3nn_0\dot{H}_{n_0}}{r} - \frac{2lnH_{n_0} + lnn_0H_{n_0} - nn_0\ddot{T}_{n_0}}{r^2} \\ & - \frac{nn_0(l+1)\dot{T}_{n_0}}{r^3} \Bigg] \end{aligned}$$

(C23)

$$x_{nn_0}^{(17)(j)}(r) = T_n^j \left[r\dot{H}_{n_0} + (n_0+5)H_{n_0} + \ddot{T}_{n_0} + \frac{3n_0\dot{T}_{n_0}}{r} - \frac{2l(n_0-1)T_{n_0}}{r^2} \right]$$

(C24)

$$x_{nn_0}^{(18)(j)}(r) = H_n^j \left[r^2 H_{n_0} + r\dot{T}_{n_0} + 2(n_0-1)T_{n_0} \right] + T_n^j \left[nH_{n_0} + \frac{n\dot{T}_{n_0}}{r} + \frac{2n(n_0-1)T_{n_0}}{r^2} \right]$$

(C25)

$$x_{nn_0}^{(19)(j)}(r) = 2T_n^j H_{n_0}$$

(C26)

$$\begin{aligned} x_{nn_0}^{(20)(j)}(r) = H_n^j & \left[2r^2\dot{H}_{n_0} + 2(n_0+1)rH_{n_0} + 2n_0\dot{T}_{n_0} + \frac{2n_0(n_0-1)T_{n_0}}{r} \right] \\ & + T_n^j \left[2n\dot{H}_{n_0} + \frac{n(n_0+2)H_{n_0}}{r} + \frac{nn_0\dot{T}_{n_0}}{r^2} \right] \end{aligned}$$

(C27)

$$x_{nn_0}^{(21)(j)}(r) = T_n^j \left[rH_{n_0} + \dot{T}_{n_0} + \frac{2(n_0-1)T_{n_0}}{r} \right]$$

(C28)

Note that terms of $x_{nn_0}^{(12)(j)}(r)$, $x_{nn_0}^{(16)(j)}(r)$, and $x_{nn_0}^{(17)(j)}(r)$ contain real Earth model expansion degree l, namely these 3 terms not only relate to n and n_0. Whereas for the consistence with previous works, these terms are still named as $x_{nn_0}^{(i)(j)}(r)$.

Appendix D: Formulae of Non-hydrostatic Pre-stress effects

According to equation 49, the non-hydrostatic pre-stress effects can be written as:

$$F_{nm}^{j}(\delta\tau) = \iiint u_i^j \nabla_k \left[\mu\gamma^1\left(\frac{\partial u_i^0}{\partial x_k} + \frac{\partial u_k^0}{\partial x_i}\right) + \lambda\gamma^1\nabla\cdot(\boldsymbol{u}^0)\delta_{ik}\right] dv \tag{D1}$$

Introducing variable $\omega_n^m = r^n Y_n^m(\theta,\phi)$, which satisfies:

$$\Delta\omega_n^m = 0$$
$$x_i\frac{\partial\omega_n^m}{\partial x_i} = n\omega_n^m \tag{D2}$$

Then u_i^j and u_i^0 can be written as,

$$u_i^j = H_n^j(r)x_i\omega_n^m + T_n^j(r)\frac{\partial\omega_n^m}{\partial x_i} \tag{D3}$$

$$u_i^0 = H_{n_0}(r)x_i\omega_{n_0}^{m_0} + T_{n_0}(r)\frac{\partial\omega_{n_0}^{m_0}}{\partial x_i} \tag{D4}$$

The definitions of $H_n^j(r)$, $T_n^j(r)$, $H_{n_0}(r)$ and $T_{n_0}(r)$ are described in Appendix C. In equation D1:

$$\gamma^1(r,\theta,\phi) = \sum_{l=0}^{N_e}\sum_{p=-l}^{l}\gamma_{lp}^1(r)Y_l^p(\theta,\phi) \tag{D5}$$

$$\frac{\partial u_i^0}{\partial x_k} + \frac{\partial u_k^0}{\partial x_i} = 2\dot{H_{n_0}}\frac{x_i x_k}{r}\omega_{n_0}^{m_0} + 2H_{n_0}\omega_{n_0}^{m_0}\delta_{ik} + \left(H_{n_0} + \frac{\dot{T}_{n_0}}{r}\right)\left(x_i\nabla_k\omega_{n_0}^{m_0} + x_k\nabla_i\omega_{n_0}^{m_0}\right) + 2T_{n_0}\nabla_i\nabla_k\omega_{n_0}^{m_0} \tag{D6}$$

$$\nabla\cdot\boldsymbol{u}^0 = D_{n_0}(r)Y_{n_0}^{m_0}(\theta,\phi) \tag{D7}$$

By substituting equations D3-D7 into equation D1 and with some manipulations, the following equation can be obtained:

$$F_{nm}^{j}(\delta\tau) = \iiint \sum_{l=0}^{N_e} \sum_{p=-l}^{l} \left(H_n^j x_i \omega_n^m + T_n^j \nabla_i \omega_n^m\right) \nabla_k \left[\mu \gamma_{lp}^1 r^{-l} \omega_l^p \left(2\dot{H}_{n_0} \frac{x_i x_k}{r} \omega_{n_0}^{m_0} + 2H_{n_0} \omega_{n_0}^{m_0} \delta_{ik} \right.\right.$$
$$\left. + \left(H_{n_0} + \frac{\dot{T}_{n_0}}{r}\right)\left(x_i \nabla_k \omega_{n_0}^{m_0} + x_k \nabla_i \omega_{n_0}^{m_0}\right) + 2T_{n_0} \nabla_i \nabla_k \omega_{n_0}^{m_0}\right)$$
$$\left. + \lambda \gamma_{lp}^1 D_{n_0} r^{-l-n_0} \omega_l^p \omega_{n_0}^{m_0} \delta_{ik}\right] dv$$
$$= \iiint \sum_{l=0}^{N_e} \sum_{p=-l}^{l} \left(H_n^j x_i \omega_n^m + T_n^j \nabla_i \omega_n^m\right) [A_1 + A_2 + A_3] dv$$

(D8)

In equation D8,

$$A_1 = \dot{\mu} \gamma_{lp}^1 \left[\frac{2\dot{H}_{n_0}}{r^l} + \frac{2H_{n_0} + n_0 H_{n_0}}{r^{l+1}} + \frac{n_0 \dot{T}_{n_0}}{r^{l+2}}\right] x_i \omega_l^p \omega_{n_0}^{m_0}$$
$$+ \mu \gamma_{lp}^1 \left[-\frac{2lH_{n_0} + n_0 l H_{n_0}}{r^{l+2}} - \frac{n_0 l \dot{T}_{n_0}}{r^{l+3}}\right] x_i \omega_l^p \omega_{n_0}^{m_0} + \dot{\mu} \gamma_{lp}^1 \left[\frac{H_{n_0}}{r^{l-1}} + \frac{\dot{T}_{n_0}}{r^l}\right] \omega_l^p \nabla_i \omega_{n_0}^{m_0}$$
$$+ \dot{\mu} \gamma_{lp}^1 \left[\frac{2T_{n_0}}{r^{l+1}}\right] x_k \omega_l^p \nabla_i \nabla_k \omega_{n_0}^{m_0} + \mu \gamma_{lp}^1 \left[-\frac{2lT_{n_0}}{r^{l+2}}\right] x_k \omega_l^p \nabla_i \nabla_k \omega_{n_0}^{m_0}$$
$$+ \mu \gamma_{lp}^1 \left[\frac{2H_{n_0}}{r^l}\right] \nabla_i \omega_l^p \omega_{n_0}^{m_0} + \mu \gamma_{lp}^1 \left[\frac{H_{n_0}}{r^l} + \frac{\dot{T}_{n_0}}{r^{l+1}}\right] x_i \nabla_k \omega_l^p \nabla_k \omega_{n_0}^{m_0}$$
$$+ \mu \gamma_{lp}^1 \left[\frac{2T_{n_0}}{r^l}\right] \nabla_k \omega_l^p \nabla_i \nabla_k \omega_{n_0}^{m_0}$$

(D9)

$$A_2 = \mu \gamma_{lp}^1 \left(\left[\frac{2\ddot{H}_{n_0}}{r^l} + \frac{8\dot{H}_{n_0} + 3n_0 \dot{H}_{n_0}}{r^{l+1}} + \frac{n_0 \ddot{T}_{n_0}}{r^{l+2}} - \frac{n_0 \dot{T}_{n_0}}{r^{l+3}}\right] x_i \omega_l^p \omega_{n_0}^{m_0}\right.$$
$$\left. + \left[\frac{6H_{n_0} + \ddot{T}_{n_0}}{r^l} + \frac{\dot{H}_{n_0}}{r^{l-1}} + \frac{3\dot{T}_{n_0}}{r^{l+1}}\right] \omega_l^p \nabla_i \omega_{n_0}^{m_0} + \left[\frac{H_{n_0}}{r^l} + \frac{3\dot{T}_{n_0}}{r^{l+1}}\right] x_k \omega_l^p \nabla_i \nabla_k \omega_{n_0}^{m_0}\right)$$

(D10)

$$A_3 = \dot{\lambda} \gamma_{lp}^1 \frac{D_{n_0}}{r^{l+n_0+1}} x_i \omega_l^p \omega_{n_0}^{m_0} + \lambda \gamma_{lp}^1 \frac{\dot{D}_{n_0}}{r^{l+n_0+1}} x_i \omega_l^p \omega_{n_0}^{m_0} - \lambda \gamma_{lp}^1 \frac{(n_0 + l) D_{n_0}}{r^{l+n_0+2}} x_i \omega_l^p \omega_{n_0}^{m_0}$$
$$+ \lambda \gamma_{lp}^1 \frac{D_{n_0}}{r^{l+n_0}} \nabla_i \omega_l^p \omega_{n_0}^{m_0} + \lambda \gamma_{lp}^1 \frac{D_{n_0}}{r^{l+n_0}} \omega_l^p \nabla_i \omega_{n_0}^{m_0}$$

(D11)

In light of equation D2, the following equations are true.

$$\begin{aligned}\left(x_i\nabla_k\omega_{n_0}^{m_0}\right)\left(\nabla_i\nabla_k\omega_n^m\right) &= \nabla_k\left(x_i\nabla_k\omega_{n_0}^{m_0}\nabla_i\omega_n^m\right) - \nabla_i\omega_n^m\nabla_k\left(x_i\nabla_k\omega_{n_0}^{m_0}\right)\\ &= \nabla_k\left(x_i\nabla_k\omega_{n_0}^{m_0}\nabla_i\omega_n^m\right) - \nabla_i\omega_n^m\left(x_i\nabla^2\omega_{n_0}^{m_0} + \nabla_k\omega_{n_0}^{m_0}\delta_{ik}\right)\\ &= \nabla_k\left(n\omega_n^m\nabla_i\omega_{n_0}^{m_0}\right) - \left(\nabla\omega_n^m, \nabla\omega_{n_0}^{m_0}\right) = (n-1)\left(\nabla\omega_n^m, \nabla\omega_{n_0}^{m_0}\right)\end{aligned}$$

$$\begin{aligned}\omega_n^m x_i x_k\nabla_i\nabla_k\omega_{n_0}^{m_0} &= \nabla_i\left(x_i x_k\omega_n^m\nabla_k\omega_{n_0}^{m_0}\right) - \nabla_k\omega_{n_0}^{m_0}\nabla_i\left(x_i x_k\omega_n^m\right)\\ &= \nabla_i\left(n_0 x_i\omega_n^m\omega_{n_0}^{m_0}\right) - \nabla_k\omega_{n_0}^{m_0}\left(3x_k\omega_n^m + x_i\delta_{ik}\omega_n^m + x_k n\omega_n^m\right)\\ &= 3n_0\omega_n^m\omega_{n_0}^{m_0} + nn_0\omega_n^m\omega_{n_0}^{m_0} + {n_0}^2\omega_n^m\omega_{n_0}^{m_0} - 4n_0\omega_n^m\omega_{n_0}^{m_0} - nn_0\omega_n^m\omega_{n_0}^{m_0}\\ &= n_0(n_0-1)\omega_n^m\omega_{n_0}^{m_0}\end{aligned}$$

(D12)

By substituting equation D12 into equation D8:

$$F_{nm}^{j}(\delta\tau) = S_1 + S_2$$

(D13)

$$\begin{aligned}S_1 = \iiint \sum_{l=0}^{N_e}\sum_{p=-l}^{l}\Bigg\{ H_n^j\Bigg[&\dot{\mu}\gamma_{lp}^1\frac{2\dot{H}_{n_0}}{r^{l-2}} + \dot{\mu}\gamma_{lp}^1\frac{2H_{n_0}+2n_0H_{n_0}}{r^{l-1}} + \dot{\mu}\gamma_{lp}^1\frac{2n_0\dot{T}_{n_0}}{r^l}\\ &+ \dot{\mu}\gamma_{lp}^1\frac{2n_0(n_0-1)T_{n_0}}{r^{l+1}} + \mu\gamma_{lp}^1\frac{2\ddot{H}_{n_0}}{r^{l-2}} + \mu\gamma_{lp}^1\frac{8\dot{H}_{n_0}+4n_0\dot{H}_{n_0}}{r^{l-1}}\\ &- \mu\gamma_{lp}^1\frac{n_0(l-n_0-5)H_{n_0}-2n_0\ddot{T}_{n_0}}{r^l} - \mu\gamma_{lp}^1\frac{n_0(l-3n_0+1)\dot{T}_{n_0}}{r^{l+1}}\\ &- \mu\gamma_{lp}^1\frac{2n_0(n_0-1)lT_{n_0}}{r^{l+2}} + \dot{\lambda}\gamma_{lp}^1\frac{D_{n_0}}{r^{l+n_0-1}} + \lambda\gamma_{lp}^1\frac{\dot{D}_{n_0}}{r^{l+n_0-1}}\Bigg]\omega_l^p\omega_n^m\omega_{n_0}^{m_0}\\ &+ H_n^j\left[\mu\gamma_{lp}^1\frac{H_{n_0}}{r^{l-2}} + \mu\gamma_{lp}^1\frac{\dot{T}_{n_0}}{r^{l-1}} + \mu\gamma_{lp}^1\frac{2(n_0-1)T_{n_0}}{r^l}\right]\omega_n^m\left(\nabla\omega_l^p, \nabla\omega_{n_0}^{m_0}\right)\Bigg\}dv\end{aligned}$$

(D14)

$$S_2 = \iiint \sum_{l=0}^{N_e} \sum_{p=-l}^{l} \Bigg\{ T_n^j \Bigg[\dot{\mu}\gamma_{lp}^1 \frac{2n\dot{H}_{n_0}}{r^l} + \dot{\mu}\gamma_{lp}^1 \frac{2nH_{n_0} + nn_0H_{n_0}}{r^{l+1}} + \dot{\mu}\gamma_{lp}^1 \frac{nn_0\dot{T}_{n_0}}{r^{l+2}} + \mu\gamma_{lp}^1 \frac{2\mathrm{n}\ddot{H}_{n_0}}{r^l}$$
$$+ \mu\gamma_{lp}^1 \frac{8n\dot{H}_{n_0} + 3nn_0\dot{H}_{n_0}}{r^{l+1}} - \mu\gamma_{lp}^1 \frac{2lnH_{n_0} + lnn_0H_{n_0} - nn_0\ddot{T}_{n_0}}{r^{l+2}}$$
$$- \mu\gamma_{lp}^1 \frac{nn_0(l+1)\dot{T}_{n_0}}{r^{l+3}} + \dot{\lambda}\gamma_{lp}^1 \frac{nD_{n_0}}{r^{l+n_0+1}} + \lambda\gamma_{lp}^1 \frac{n\dot{D}_{n_0}}{r^{l+n_0+1}}$$
$$- \lambda\gamma_{lp}^1 \frac{n(n_0+l)D_{n_0}}{r^{l+n_0+2}} \Bigg] \omega_l^p \omega_n^m \omega_{n_0}^{m_0}$$
$$+ T_n^j \Bigg[\dot{\mu}\gamma_{lp}^1 \frac{H_{n_0}}{r^{l-1}} + \dot{\mu}\gamma_{lp}^1 \frac{\dot{T}_{n_0}}{r^l} + \dot{\mu}\gamma_{lp}^1 \frac{2(n_0-1)T_{n_0}}{r^{l+1}} + \mu\gamma_{lp}^1 \frac{\dot{H}_{n_0}}{r^{l-1}}$$
$$+ \mu\gamma_{lp}^1 \frac{(n_0+5)H_{n_0} + \ddot{T}_{n_0}}{r^l} + \mu\gamma_{lp}^1 \frac{3n_0\dot{T}_{n_0}}{r^{l+1}} - \mu\gamma_{lp}^1 \frac{2l(n_0-1)T_{n_0}}{r^{l+2}}$$
$$+ \lambda\gamma_{lp}^1 \frac{D_{n_0}}{r^{l+n_0}} \Bigg] \omega_l^p \left(\nabla\omega_n^m, \nabla\omega_{n_0}^{m_0}\right) + T_n^j \left[\mu\gamma_{lp}^1 \frac{2H_{n_0}}{r^l} + \lambda\gamma_{lp}^1 \frac{D_{n_0}}{r^{l+n_0}} \right] \omega_{n_0}^{m_0} \left(\nabla\omega_l^p, \nabla\omega_n^m\right)$$
$$+ T_n^j \left[\mu\gamma_{lp}^1 \frac{nH_{n_0}}{r^l} + \mu\gamma_{lp}^1 \frac{n\dot{T}_{n_0}}{r^{l+1}} + \mu\gamma_{lp}^1 \frac{2n(n_0-1)T_{n_0}}{r^{l+2}} \right] \omega_n^m \left(\nabla\omega_l^p, \nabla\omega_{n_0}^{m_0}\right) \Bigg\} dv$$

(D15)

Consequently,

$$F_{nm}^j(\delta\tau) = \iiint \sum_{l=0}^{N_e} \sum_{p=-l}^{l} \frac{1}{r^l} \Big\{ \lambda\gamma_{lp}^1(r) x_{nn_0}^{(12)(j)}(r) \omega_l^p \omega_n^m \omega_{n_0}^{m_0} + \lambda\gamma_{lp}^1(r) x_{nn_0}^{(13)(j)}(r) \omega_l^p \left(\nabla\omega_n^m, \nabla\omega_{n_0}^{m_0}\right)$$
$$+ \lambda\gamma_{lp}^1(r) x_{nn_0}^{(14)(j)}(r) \omega_{n_0}^{m_0} \left(\nabla\omega_l^p, \nabla\omega_n^m\right) + \dot{\lambda}\gamma_{lp}^1(r) x_{nn_0}^{(15)(j)}(r) \omega_l^p \omega_n^m \omega_{n_0}^{m_0}$$
$$+ \mu\gamma_{lp}^1(r) x_{nn_0}^{(16)(j)}(r) \omega_l^p \omega_n^m \omega_{n_0}^{m_0} + \mu\gamma_{lp}^1(r) x_{nn_0}^{(17)(j)}(r) \omega_l^p \left(\nabla\omega_n^m, \nabla\omega_{n_0}^{m_0}\right)$$
$$+ \mu\gamma_{lp}^1(r) x_{nn_0}^{(18)(j)}(r) \omega_n^m \left(\nabla\omega_l^p, \nabla\omega_{n_0}^{m_0}\right) + \mu\gamma_{lp}^1(r) x_{nn_0}^{(19)(j)}(r) \omega_{n_0}^{m_0} \left(\nabla\omega_l^p, \nabla\omega_n^m\right)$$
$$+ \dot{\mu}\gamma_{lp}^1(r) x_{nn_0}^{(20)(j)}(r) \omega_l^p \omega_n^m \omega_{n_0}^{m_0} + \dot{\mu}\gamma_{lp}^1(r) x_{nn_0}^{(21)(j)}(r) \omega_l^p \left(\nabla\omega_n^m, \nabla\omega_{n_0}^{m_0}\right) \Big\} dv$$

(D16)

The expressions of $x_{nn_0}^{(i)(j)}(r)$ $(i = 12, \ldots, 21)$ shown in Appendix C can be obtained with simple manipulations. The terms containing ω in the equation D16 can be transformed into:

$$\iiint \omega_l^p \omega_n^m \omega_{n_0}^{m_0} f(r)\, dv = \iiint r^{l+n+n_0+2} Y_l^p Y_n^m Y_{n_0}^{m_0} f(r)\, dSdr$$
$$= A_{lpnmn_0m_0} \int_0^1 r^{l+n+n_0+2} f(r)\, dr$$

(D17)

$$\iiint \omega_l^p\left(\nabla\omega_n^m,\nabla\omega_{n_0}^{m_0}\right)f(r)\,dv=\iiint \omega_l^p\frac{n\omega_n^m}{x_i}\frac{n_0\omega_{n_0}^{m_0}}{x_i}f(r)\,dv=nn_0\iiint \omega_l^p\omega_n^m\omega_{n_0}^{m_0}\frac{f(r)}{r^2}dv$$
$$=nn_0\iiint r^{l+n+n_0}Y_l^pY_n^mY_{n_0}^{m_0}f(r)\,dSdr=nn_0A_{lpnmn_0m_0}\int_0^1 r^{l+n+n_0}f(r)\,dr$$

(D18)

$$\iiint \omega_l^p\nabla_i\nabla_k\omega_n^m\nabla_i\nabla_k\omega_{n_0}^{m_0}f(r)\,dv=\iiint \omega_l^p\nabla_i\left(\frac{n\omega_n^m}{x_k}\right)\nabla_i\left(\frac{n_0\omega_{n_0}^{m_0}}{x_k}\right)f(r)\,dv$$
$$=nn_0\iiint \omega_l^p\frac{\nabla_i\omega_n^mx_k-\omega_n^m\delta_{ik}}{{x_k}^2}\frac{\nabla_i\omega_{n_0}^{m_0}x_k-\omega_{n_0}^{m_0}\delta_{ik}}{{x_k}^2}f(r)\,dv$$
$$=nn_0(nn_0-n_0-n+3)\iiint r^{l+n+n_0-2}Y_l^pY_n^mY_{n_0}^{m_0}f(r)\,dSdr$$
$$=nn_0(nn_0-n_0-n+3)A_{lpnmn_0m_0}\int_0^1 r^{l+n+n_0-2}f(r)\,dr$$

(D19)

Finally, equation 50 is obtained.

Appendix E: Final Formulae for Effects of Lateral Inhomogeneity

By substituting equation 33 into equation 15:

$$\Delta g(\theta,\phi)=\sum_{n=0}^{\infty}\sum_{m=-n}^{n}\frac{1}{c(n,m)}\left[(n+1)F^{j=3}(\delta\rho,\delta\mu,\delta\lambda,\delta\tau)-2F^{j=1}(\delta\rho,\delta\mu,\delta\lambda,\delta\tau)\right]Y_n^m(\theta,\phi)$$

(E1)

The perturbation of λ is taken for example. By substituting equation 36 into equation E1,

$$\Delta g_\lambda(\theta,\phi)=-\sum_{n=0}^{\infty}\sum_{m=-n}^{n}\sum_{l=0}^{N_e}\sum_{p=-l}^{l}\frac{A_{lpnmn_0m_0}}{c(n,m)}Y_n^m(\theta,\phi)\int_0^1\lambda_{lp}(r)\left[(n+1)x_{nn_0}^{(1)(j=3)}(r)-2x_{nn_0}^{(1)(j=1)}(r)\right]dr$$
$$=\sum_{n=0}^{\infty}\sum_{m=-n}^{n}\sum_{l=0}^{N_e}\sum_{p=-l}^{l}\frac{E_{lpnmn_0m_0}}{c(n,m)}I(p,m,m_0)Y_n^m(\theta,\phi)\int_0^1\lambda_{lp}(r)y_n(r)dr$$

(E2)

$$y_n(r)=2x_{nn_0}^{(1)(j=1)}(r)-(n+1)x_{nn_0}^{(1)(j=3)}(r)$$

(E3)

Therein, the treatments on $E_{lpnmn_0m_0}$ and $I(p,m,m_0)$ can be found in Appendix B.

As discussed by Molodenskii & Kramer (1980), $I(p,m,m_0) \neq 0$ only when $p = m \pm m_0$. Besides, $E_{lpnmn_0m_0} = 0$ if l, n, and n_0 do not satisfy a triangle inequality. The integration of dr start from the core-mantle boundary, rather than the core of Earth, to the surface. So the equation E2 simplifies as,

$$\Delta g_\lambda(\theta,\phi) = \sum_{l=0}^{N_e} \sum_{p=-l}^{l} \sum_{n=|l-n_0|}^{l+n_0} \frac{E_{lpnmn_0m_0}}{c(n,p \pm m_0)} I(p,p \pm m_0,m_0) Y_n^{p \pm m_0}(\theta,\phi) \int_b^1 \lambda_{lp}(r) y_n(r) dr$$

By replacing $\lambda_{lp}(r)$ with $\alpha_{lp}(r)$, $\beta_{lp}(r)$, and $\gamma_{lp}^1(r)$ with the help of equation 51:

$$\Delta g_\lambda(\theta,\phi) = \sum_{l=0}^{N_e} \sum_{p=-l}^{l} \sum_{n=|l-n_0|}^{l+n_0} \frac{E_{lpn(p \pm m_0)n_0m_0}}{c(n,p \pm m_0)} I(p,p \pm m_0,m_0) Y_n^{p \pm m_0}(\theta,\phi) \int_b^1 y_n(r) \big[2(\lambda + 2\mu)\alpha_{lp}(r) - 4\mu\beta_{lp}(r) + \lambda\gamma_{lp}^1(r)\big] dr \quad \text{(E4)}$$

Similarly, the expressions for $\delta\mu$, $\delta\rho$, and $\delta\tau$ are,

$$\Delta g_\mu(\theta,\phi) = \sum_{l=0}^{N_e} \sum_{p=-l}^{l} \sum_{n=|l-n_0|}^{l+n_0} \frac{E_{lpn(p \pm m_0)n_0m_0}}{c(n,p \pm m_0)} I(p,p \pm m_0,m_0) Y_n^{p \pm m_0}(\theta,\phi) \int_b^1 z_n(r) \big[2\mu\beta_{lp}(r) + \mu\gamma_{lp}^1(r)\big] dr \quad \text{(E5)}$$

$$\Delta g_\rho(\theta,\phi) = \sum_{l=0}^{N_e} \sum_{p=-l}^{l} \sum_{n=|l-n_0|}^{l+n_0} \frac{E_{lpn(p \pm m_0)n_0m_0}}{c(n,p \pm m_0)} I(p,p \pm m_0,m_0) Y_n^{p \pm m_0}(\theta,\phi) \int_b^1 \rho(r) \big[q_n^1(r)\gamma_{lp}^1(r) + q_n^2(r)\gamma_{lp}^2(r) + q_n^3(r)\gamma_{lp}^3(r)\big] dr \quad \text{(E6)}$$

$$\Delta g_\tau(\theta,\phi) = -\sum_{l=0}^{N_e} \sum_{p=-l}^{l} \sum_{n=|l-n_0|}^{l+n_0} \frac{E_{lpn(p \pm m_0)n_0m_0}}{c(n,p \pm m_0)} I(p,p \pm m_0,m_0) Y_n^{p \pm m_0}(\theta,\phi) \int_b^1 \gamma_{lp}^1(r) \big[\lambda q_n^4(r) + \dot{\lambda} q_n^5(r) + \mu q_n^6(r) + \dot{\mu} q_n^7(r)\big] dr \quad \text{(E7)}$$

In equations E5-E7,

$$z_n(r) = r^{n+n_0}\Big[2x_{nn_0}^{(2)(j=1)}(r) - (n+1)x_{nn_0}^{(2)(j=3)}(r) + nn_0\left(2x_{nn_0}^{(3)(j=1)}(r) - (n+1)x_{nn_0}^{(3)(j=3)}(r)\right) + nn_0(nn_0 - n_0 - n + 3)\left(2x_{nn_0}^{(4)(j=1)}(r) - (n+1)x_{nn_0}^{(4)(j=3)}(r)\right)\Big]$$

(E8)

$$q_n^1(r) = 2x_{nn_0}^{(5)(j=1)}(r) - (n+1)x_{nn_0}^{(5)(j=3)}(r) + nn_0\left(2x_{nn_0}^{(6)(j=1)}(r) - (n+1)x_{nn_0}^{(6)(j=3)}(r)\right)$$

(E9)

$$q_n^2(r) = 2x_{nn_0}^{(7)(j=1)}(r) - (n+1)x_{nn_0}^{(7)(j=3)}(r) - l\left(2x_{nn_0}^{(8)(j=1)}(r) - (n+1)x_{nn_0}^{(8)(j=3)}(r)\right) + nn_0\left(2x_{nn_0}^{(9)(j=1)}(r) - (n+1)x_{nn_0}^{(9)(j=3)}(r)\right) + nl\left(2x_{nn_0}^{(10)(j=1)}(r) - (n+1)x_{nn_0}^{(10)(j=3)}(r)\right)$$

(E10)

$$q_n^3(r) = 2x_{nn_0}^{(11)(j=1)}(r) - (n+1)x_{nn_0}^{(11)(j=3)}(r)$$

(E11)

$$q_n^4(r) = r^{n+n_0}\Big[2x_{nn_0}^{(12)(j=1)}(r) - (n+1)x_{nn_0}^{(12)(j=3)}(r) + nn_0\left(2x_{nn_0}^{(13)(j=1)}(r) - (n+1)x_{nn_0}^{(13)(j=3)}(r)\right) + nl\left(2x_{nn_0}^{(14)(j=1)}(r) - (n+1)x_{nn_0}^{(14)(j=3)}(r)\right)\Big]$$

(E12)

$$q_n^5(r) = r^{n+n_0}\left[2x_{nn_0}^{(15)(j=1)}(r) - (n+1)x_{nn_0}^{(15)(j=3)}(r)\right]$$

(E13)

$$q_n^6(r) = r^{n+n_0}\Big[2x_{nn_0}^{(16)(j=1)}(r) - (n+1)x_{nn_0}^{(16)(j=3)}(r) + nn_0\left(2x_{nn_0}^{(17)(j=1)}(r) - (n+1)x_{nn_0}^{(17)(j=3)}(r)\right) + n_0 l\left(2x_{nn_0}^{(18)(j=1)}(r) - (n+1)x_{nn_0}^{(18)(j=3)}(r)\right) + nl\left(2x_{nn_0}^{(19)(j=1)}(r) - (n+1)x_{nn_0}^{(19)(j=3)}(r)\right)\Big]$$

(E14)

$$q_n^7(r) = r^{n+n_0}\left[2x_{nn_0}^{(20)(j=1)}(r) - (n+1)x_{nn_0}^{(20)(j=3)}(r) + nn_0\left(2x_{nn_0}^{(21)(j=1)}(r) - (n+1)x_{nn_0}^{(21)(j=3)}(r)\right)\right] \quad \text{(E15)}$$

Equations E4 and E5 can be transformed into the forms relating to seismic wave velocity disturbance, namely equations 54 and 55.

References

Balmino, G., Lambeck, K., & Kaula, W. M. (1973). A spherical harmonic analysis of the Earth's topography. *Journal of Geophysical Research*, *78*(2), 478-481. https://doi.org/10.1029/JB078i002p00478

Boy, J. P., Llubes, M., Hinderer, J., & Florsch, N. (2003). A comparison of tidal ocean loading models using superconducting gravimeter data. *Journal of Geophysical Research: Solid Earth*, *108*(B4). https://doi.org/10.1029/2002JB002050

Dahlen, F. A. (1972). Elastic dislocation theory for a self-gravitating elastic configuration with an initial static stress field. *Geophysical Journal International*, *28*(4), 357-383. https://doi.org/10.1111/j.1365-246X.1972.tb06798.x

Dehant, V. (1987). Tidal parameters for an inelastic Earth. *Physics of the Earth and Planetary Interiors*, *49*(1-2). 97-116. https://doi.org/10.1016/0031-9201(87)90134-8

Dehant, V., Defraigne, P., & Wahr, J. M. (1999). Tides for a convective Earth. *Journal of Geophysical Research: Solid Earth*, *104*(B1), 1035-1058. https://doi.org/10.1029/1998JB900051

de Vries, D., & Wahr, J. M. (1991). The effects of the solid inner core and non-hydrostatic structure on the Earth's forced nutations and Earth tides. *Journal of Geophysical Research: Solid Earth*, *96*(B5), 8275-8293. https://doi.org/10.1029/90JB01958

Dziewonski, A. M., & Anderson, D. L. (1981). Preliminary reference Earth model. *Physics of the Earth and Planetary Interiors*, *25*(4), 297-356. doi: 10.1016/0031- 9201(81)90046-7

Eanes, R. J., & Bettadpur, S. (1996). The CSR3. 0 global ocean tide model: diurnal and semi-diurnal ocean tides from TOPEX/POSEIDON altimetry. *The University of Texas Center for Space Research*.

Farrell, W. E. (1972). Deformation of the Earth by surface loads. *Reviews of Geophysics*, *10*(3), 761-797. https://doi.org/10.1029/RG010i003p00761

Fores, B., Champollion, C., Moigne, N. L., Bayer, R., & Chery, J. (2016). Assessing the precision of the iGrav superconducting gravimeter for hydrological models and karstic hydrological process identification. *Geophysical Journal International*, *ggw396*, 269-280. https://doi.org/10.1093/gji/ggw396

Fu, G., & Sun, W. (2007). Effects of lateral inhomogeneity in a spherical Earth on gravity Earth tides. *Journal of Geophysical Research: Solid Earth*, *112*(B6). https://doi.org/10.1029/2006JB004512

Fu, G., & Sun, W. (2008). Surface coseismic gravity changes caused by dislocations in a three-dimensional heterogeneous Earth. *Geophysical Journal International*, *172*(2), 479-503. https://doi.org/10.1111/j.1365-246X.2007.03684.x

Geller, R. J. (1988). Elastodynamics in a laterally heterogeneous, self-gravitating body. *Geophysical Journal International*, *94*(2), 271-283. https://doi.org/10.1111/j.1365-246X.1988.tb05901.x

Gilbert, F., & Dziewonski, A. M. (1975). An application of normal mode theory to the retrieval of structural parameters and source mechanisms from seismic spectra. *Philosophical Transactions of the Royal Society A, Mathematical, Physical and Engineering Sciences*, *278*(1280), 187-269. https://doi.org/10.1098/rsta.1975.0025

Karato, S. I. (1993). Importance of anelasticity in the interpretation of seismic tomography. *Geophysical Research Letters*, *20*(15), 1623-1626. https://doi.org/10.1029/93GL01767

Lau, H. C., & Faul, U. H. (2019). Anelasticity from seismic to tidal timescales: Theory and obser vations. *Earth and Planetary Science Letters*, *508*, 18-29. https://doi.org/10.1016/j.epsl.2018.12.009

Lau, H. C., Yang, H. Y., Tromp, J., Mitrovica, J. X., Latychev, K., & Al-Attar, D. (2015). A normal mode treatment of semi-diurnal body tides on an aspherical, rotating and anelastic Earth. *Geophysical Journal International*, *202*(2), 1392-1406. doi: 10.1093/gji/ggv227

Longman, I. M., (1963). A Green's function for determining the deformation of the Earth under surface mass loads: 2. computations and numerical results. *Journal of Geophysical Research*, *68*(2), 485-496. https://doi.org/10.1029/JZ068i002p00485

Love, A. E. H. (1909). The yielding of the Earth to disturbing forces. *Proceedings of the Royal Society A, Mathematical, Physical and Engineering Sciences*, *82*(551), 73-88. https://doi.org/10.1098/rspa.1909.0008

Maitra, M., & Al-Attar, D. (2020). On the stress dependence of the elastic tensor. *arXiv preprint arXiv:2007.13283*. https://arxiv.org/abs/2007.13283

Métivier, L., Greff-Lefftz, M., & Diament, M. (2006). Mantle lateral variations and elastogravitational deformations–I. Numerical modelling. *Geophysical Journal International*, *167*(3), 1060-1076. https://doi.org/10.1111/j.1365-246X.2006.03159.x

Métivier, L., Greff-Lefftz, M., & Diament, M. (2007). Mantle lateral variations and elastogravitational deformations–II. Possible effects of a superplume on body tides. *Geophysical Journal International*, *168*(3), 897-903. https://doi.org/10.1111/j.1365-246X.2006.03309.x

Molodenskiy, S. M. (1977). The influence of horizontal inhomogeneities in the mantle on the amplitude of tidal oscillations. *Izvestiya, Physics of the Solid Earth*, *13*, 77-80.

Molodenskiy, S. M. (1980). The effect of lateral heterogeneities upon the tides. *BIM Fevrier*, *80*, 4833-4850.

Molodenskii, S. M., & Kramer, M. V. (1980). The influence of large-scale horizontal inhomogeneities in the mantle on Earth tides. *Izvestiya, Earth Physics*, *16*, 1-11.

Petrov, L., & Boy, J. P. (2004). Study of the atmospheric pressure loading signal in very long baseline interferometry observations. *Journal of Geophysical Research: Solid Earth*, *109*(B3). https://doi.org/10.1029/2003JB002500

Qin, C., Zhong, S., & Wahr, J. (2014). A perturbation method and its application: elastic tidal response of a laterally heterogeneous planet. *Geophysical Journal International*, *199*(2), 631-647. https://doi.org/10.1093/gji/ggu279

Saito, M. (1967). Excitation of free oscillations and surface waves by a point source in a vertically heterogeneous Earth. *Journal of Geophysical Research*, *72*(14), 3689-3699. https://doi.org/10.1029/JZ072i014p03689

Simmons, N. A., Forte, A. M., Boschi, L., & Grand, S. P. (2010). GyPSuM: A joint tomographic model of mantle density and seismic wave speeds. *Journal of Geophysical Research: Solid Earth*, *115*(B12). https://doi.org/10.1029/2010JB007631

Sun, H., Zhang, H., Xu, J., Chen, X., Zhou, J., & Zhang, M. (2019). Influences of the Tibetan plateau on tidal gravity detected by using SGs at Lhasa, Lijiang and Wuhan Stations in China. *Terrestrial, Atmospheric and Oceanic Sciences*, *30*(1), 139-149. doi: 10.3319/TAO.2019.02.14.01

Sun, W., & Okubo, S. (1993). Surface potential and gravity changes due to internal dislocations in a spherical Earth—I. Theory for a point dislocation. *Geophysical Journal International*, *114*(3), 569-592. https://doi.org/10.1111/j.1365-246X.1993.tb06988.x

Takeuchi, H., & Saito, M. (1972). Seismic surface waves. *Methods in Computational Physics: Advances in Research and Applications*, *11*, 217-295. https://doi.org/10.1016/B978-0-12-460811-5.50010-6

Trabant, C., Hutko, A. R., Bahavar, M., Karstens, R., Ahern, T., & Aster, R. (2012). Data products at the IRIS DMC: Stepping stones for research and other applications. *Seismological Research Letters*, *83*(5), 846-854. https://doi.org/10.1785/0220120032

Tromp, J., & Trampert, J. (2018). Effects of induced stress on seismic forward modelling and inversion. *Geophysical Journal International*, *213*(2), 851-867. https://doi.org/10.1093/gji/ggy020

Vermeersen, L. L. A., & Vlaar, N. J. (1991). The gravito-elastodynamics of a pre-stressed elastic Earth. *Geophysical Journal International*, *104*(3), 555-563. https://doi.org/10.1111/j.1365-246X.1991.tb05701.x

Wahr, J. M. (1981). Body tides on an elliptical, rotating, elastic and oceanless Earth. *Geophysical Journal International*, *64*(3), 677-703. https://doi.org/10.1111/j.1365-246X.1981.tb02690.x

Wahr, J., & Bergen, Z. (1986). The effects of mantle anelasticity on nutations, Earth tides, and tidal variations in rotation rate. *Geophysical Journal International*, *87*(2), 633-668. https://doi.org/10.1111/j.1365-246X.1986.tb06642.x

Wang, R. (1991). Tidal Deformations on a Rotating, Spherically Asymmetric, Viscoelastic and Laterally Heterogeneous Earth, (Doctoral dissertation). Retrieved from Peter Lang. Frankfurt am Main

Yuan, L., Chao, B. F., Ding, X., & Zhong, P. (2013). The tidal displacement field at Earth's surface determined using global GPS observations. *Journal of Geophysical Research: Solid Earth, 118*(5), 2618-2632. http://doi.org/10.1002/jgrb.50159